

Lena Ana Mischkulnig

**PDGF-BB induced proliferation of parenchymal
fibroblasts is Angptl4 dependent**

MASTER'S THESIS

to achieve the university degree of

Master of Science

Master's degree programme: Molecular Microbiology

submitted to

Graz University of Technology

Supervisor

Prof. Dr. Andrea OLSCHESKI

and

PD. Dr. Grazyna KWAPISZEWSKA

Ludwig Boltzmann Institut for Lung Vascular Research

Medical University of Graz

Graz, January 2016

AFFIDAVIT

I declare that I have authored this thesis independently, that I have not used other than the declared sources/resources, and that I have explicitly indicated all material which has been quoted either literally or by content from the sources used. The text document uploaded to TUGRAZonline is identical to the present master's thesis dissertation.

Date

Signature

Danksagung

An dieser Stelle möchte ich all jenen danken, die mich im Rahmen meiner Masterarbeit unterstützt haben.

Zuerst möchte ich einen besonderen Dank an meine zwei Betreuerinnen Prof. Dr. Andrea Olschewski und PD. Dr. Grazyna Kwapiszewska aussprechen, die mir meine Masterarbeit am Ludwig Botzmann Institut für Lungengefäßforschung ermöglicht haben und für Ihre Unterstützung. Im Weiteren möchte ich Dr. Julia Hoffmann danken durch ihre Anregungen konnte ich meine Arbeit kontinuierlich verbessern. Ein besonderer Dank gilt Lisa Oberreiter, M.Sc und Anna Gungl, M.Sc., welche mich fachlich, wie auch persönlich unterstützt haben und mir immer wieder Kraft gaben. Ich möchte auch all den anderen Kollegen danken, die mir täglich zu Seite standen.

Ein ganz besonders Dank gehört meiner Familie, die mich während meines gesamten Studiums unterstützt hat, mir immer motivierend beiseite gestanden ist und mir mit Geduld und Ratschlägen über alle Höhen und Tiefen hinweg geholfen hat.

Danken möchte ich außerdem meinen FreundInnen und StudienkollegInnen, welche mich immer unterstützt und motiviert haben.

Table of Contents

Abbreviations and Definitions	6
List of figures	10
List of tables	11
Zusammenfassung.....	12
Abstract.....	13
1 Introduction	14
1.1 Interstitial lung disease.....	14
1.2 Fibroblasts	14
1.3 Platelet-derived growth factor and its signaling.....	14
1.4 Angiopoietin-like 4.....	16
1.4.1 Structure of Angiopoietin-like 4	17
1.4.2 Function of Angiopoietin-like 4	18
1.4.3 Angiopoietin-like 4 in disease	18
2 Aim of the study	20
3 Material and Methods	21
3.1 Cell culture.....	21
3.1.1 Primary cells in cell culture.....	21
3.1.2 Transfection of primary cells.....	21
3.1.3 Stimulation of primary cells.....	23
3.1.4 Proliferation assay.....	23
3.2 Molecular biology techniques	24
3.2.1 Isolation of RNA.....	24
3.2.2 cDNA synthesis	24
3.2.3 Real-time-PCR	25
3.2.4 Protein isolation.....	26
3.2.5 SDS-Page and western blot.....	27
3.2.6 Coomassie blue staining	31
3.3 Cloning.....	32
3.3.1 Media.....	32
3.3.2 Template cDNA.....	32

3.3.3	Establishment of the cJun-fragment.....	33
3.3.4	Electrophoresis.....	35
3.3.5	Purification of PCR products.....	35
3.3.6	Restriction.....	35
3.3.7	Gel Extraction	36
3.3.8	Ligation.....	37
3.3.9	Transformation.....	37
3.3.10	Overnight culture.....	38
3.3.11	Miniprep	38
3.3.12	Restriction.....	38
3.3.13	Maxiprep.....	39
3.3.14	Sequencing.....	40
3.4	Statistic analysis.....	40
4	Results	41
4.1	Expression of Angptl4 is elevated upon PDGF-BB stimulation in human parenchymal fibroblasts	41
4.2	MEK1/2 regulates the expression of Angptl4 in human parenchymal fibroblasts..	43
4.3	Cloning of the transcription factors Fra-2, JunB and cJun	44
4.3.1	Cloning of cJun in the expression vector (pcDNA3.1 (+))	44
4.3.2	Transformation of vector complexes in E.coli.....	46
4.4	AP-1 complex has no significant effect on Angptl4 expression in human parenchymal fibroblasts	47
4.5	Angptl4 has an effect on proliferation of human parenchymal fibroblasts	48
5	Discussion	50
5.1	Outlook.....	53
6	Supplement	54
7	Reference.....	58

Abbreviations and Definitions

Δ	Delta
$^{\circ}\text{C}$	Grad Celsius
μl	Microliter
μM	Micromolar
Akt	Protein kinase B
ANGPTL	Angiopoietin-like
Angptl4	Angiopoietin-like 4
ANOVA	Analysis of variance
AP-1	Activator protein 1
APS	Ammonium persulfate
B2M	Beta-2-microglobulin
bp	Base pairs
C	C-terminal domain of Angptl4
cDNA	Complementary DNA
CO_2	Carbon dioxide
Ct	Cycle threshold
Ctrl	Control
CVD	Cardiovascular disease
dH ₂ O	Distilled water
DMEM	Dulbecco's modified Eagle's medium
DNA	Deoxyribonuclein acid
E.coli	Escherichia coli
ECL	Enhanced chemiluminescence

ECM	Extracellular matrix
EDTA	Ethylenediaminetetraacetic acid
Erk	Extracellular-signal-regulated kinase
FCS	Fetal calf serum
Full	Full length of Angptl4
fw	Forward
g	Gravitation force
h	Hour
HRP	Horseradish peroxidase
Ig	Immunoglobulin
IPF	Idiopathic pulmonary fibrosis
JNK	c-Jun N-terminal kinase
kb	Kilo base
kDa	Kilo Dalton
l	Liter
LB	Lysogeny broth
LPL	Lipoprotein lipase
MAPK	Mitogen-activated protein kinase
MEK	Mitogen-activated protein kinase kinase
MetOH	Methyl alcohol
min	Minute
ml	Milliliter
mM	Millimolar
mRNA	Messenger ribonucleic acid
N	N-terminal domain of Angptl4
n/#	Number

NaCl	Sodium chloride
ng	Nanogram
nm	Nanometer
nt	Non treated
ONC	Overnight culture
p38	Mitogen-activated protein kinase
PBGD	Porphobilinogen deaminase
PCR	Polymerase chain reaction
PDGF	Platelet-derived growth factor
PDGF-BB	Platelet-derived growth factor- BB
PI3K	Phosphoinositide 3-kinase
PKC	Protein kinase C
PPAR	Peroxisome proliferation activators
PRO	Pro-protein
PVDF	Polyvinylidene difluoride
Raf-1	Rapidly accelerated fibrosarcoma
Ras	GTPase
RNA	Ribonucleic acid
RNase	Ribonuclease
RT	Room temperature
rv	Reverse
s	Second
SDS	Sodium dodecyl sulfate
SEM	Standard error of the mean
siRNA	Small interfering RNA
SOC	Super optimal broth with catabolite

	repression
SP	Signal peptide
std	Standard
TAE	Tris-acetate-EDTA
TBS-T	Tris-buffered saline + Tween 20
TEMED	<i>N,N,N,N</i> -Tetramethylethylenediamine
U	Unit
UV	Ultraviolet
V	Volt

List of figures

<i>Figure 1.1: Structure of PDGF-B</i>	15
<i>Figure 1.2: Signaling of PDGF</i>	16
<i>Figure 1.3: Structure of Angptl4</i>	17
<i>Figure 1.4: An overview of pathophysiological mechanisms in which Angptl4 plays a role</i>	18
<i>Figure 1.5: Mechanism of Angptl4 in tissue remodelling</i>	19
<i>Figure 2.1: Schematic representation of possible Angptl4 expression regulation in human parenchymal fibroblasts</i>	20
<i>Figure 3.1: The designed primers, which were used for the gradient PCR</i>	33
<i>Figure 4.1: Expression of Angptl4 is elevated upon PDGF-BB stimulation in human parenchymal fibroblasts</i>	42
<i>Figure 4.2: Human parenchymal fibroblasts secrete cleaved Angptl4</i>	43
<i>Figure 4.3: MEK1/2 regulates the expression of Angptl4 in human parenchymal fibroblasts</i>	44
<i>Figure 4.4: The cJun fragment has a size of 1000bp</i>	45
<i>Figure 4.5: Establishment of the cJun fragment from a human cDNA</i>	45
<i>Figure 4.6: Gel electrophoresis showed the pcDNA3.1(+) and cJun fragment cut by EcoRI and XhoI</i>	46
<i>Figure 4.7: The Restriction result of CMV-hu-Fra2 [pcDNA3] cut by AvaII and pGEMT-hu-JunB cut by BsaHI</i>	47
<i>Figure 4.8: Silencing of AP-1 complex has no significant effect on Angptl4 expression in human parenchymal fibroblasts</i>	48
<i>Figure 4.9: siAngptl4 decreased the proliferation of human parenchymal fibroblasts</i>	49
<i>Figure 5.1: Schematic representation of the upstream signaling from Angptl4 in human fibroblasts</i>	52
<i>Figure 5.2: Schematic figure how Angptl4 could be involved in the pathogenesis of IPF</i>	53

List of tables

<i>Table 1: Media used for cell culture.....</i>	<i>21</i>
<i>Table 2: siRNA used for transfection of primary cells.....</i>	<i>22</i>
<i>Table 3: Inhibitors utilized for cell stimulation.</i>	<i>23</i>
<i>Table 4: Components and volumes used for the iScript cDNA synthesis.....</i>	<i>24</i>
<i>Table 5: PCR reaction protocol for iScript cDNA synthesis.....</i>	<i>25</i>
<i>Table 6: Primer sequences.....</i>	<i>25</i>
<i>Table 7: The Real-time PCR temperature program.</i>	<i>26</i>
<i>Table 8: Compounds to produce one 10% SDS polyacrylamide gels.</i>	<i>28</i>
<i>Table 9: Buffers used for SDS-Page and western blot.</i>	<i>29</i>
<i>Table 10: Antibodies for western blot.....</i>	<i>30</i>
<i>Table 11 Solutions used for Coomassie Blue staining.....</i>	<i>31</i>
<i>Table 12: Media used for cloning.</i>	<i>32</i>
<i>Table 13: Components used for the RevertAid First Strand cDNA Synthesis.....</i>	<i>32</i>
<i>Table 14: PCR temperature program.</i>	<i>33</i>
<i>Table 15: Components used for the AmpliTaq Gold® 360 Master Mix PCR reaction.</i>	<i>34</i>
<i>Table 16: PCR temperature program for the gradient PCR.....</i>	<i>34</i>
<i>Table 17: Primer sequences utilized for the establishment of the cJun fragment. The highlighted letters are the recognition sites for the restriction enzymes EcoRI and XhoI.....</i>	<i>34</i>
<i>Table 18: Buffer used for the gel electrophoresis.....</i>	<i>35</i>
<i>Table 19: Restriction enzymes utilized for cutting the cJun fragment and plasmid (pcDNA3.1 (+))......</i>	<i>36</i>
<i>Table 20: Components for the restriction reaction.....</i>	<i>36</i>
<i>Table 21: Components for the plasmid and insert ligation.....</i>	<i>37</i>
<i>Table 22: Vectors used for the transformation in E.coli.....</i>	<i>37</i>
<i>Table 23: Restriction enzymes used for the restriction reaction. Y: C or T; R: A or G; W: A or T.....</i>	<i>39</i>
<i>Table 24: Components used for the restriction reaction.....</i>	<i>39</i>
<i>Table 25: Primer created for the sequencing of the vectors.</i>	<i>40</i>

Zusammenfassung

Idiopathische Lungenfibrose (IPF) ist eine irreversible und oft tödliche Lungenerkrankung unbekannter Ursache. Das Lungengewebe wird dick, steif und vernarbt/fibrotisch mit der Zeit. Die Pathogenese von IPF ist noch schlecht erforscht. Man weiß, dass extrazelluläre Matrix (ECM) Proteine an der Pathobiologie von IPF beteiligt sind. Angiopoietin-like 4 (ANGPTL4) ist eines dieser ECM Proteine und könnte in die Entstehung von IPF beitragen. In der vorliegenden Studie wollten wir herausfinden, welche Rolle ANGPTL4 in der Pathogenese von Lungenfibrose spielt. ANGPTL4 bei IPF wurde in diversen *in vitro* Experimenten untersucht. Isolierte parenchymale Fibroblasten dienten als Werkzeuge um den Signalweg zu beschreiben. Wir haben beobachtet, dass der Platelet-Derived Growth Factor (PDGF-BB) zu einem zeitabhängigen Anstieg der ANGPTL4 Expression in humanen parenchymalen Fibroblasten führt. Diese PDGF-BB vermittelte Angpl4 Expression wird über den Ras / MEK / ERK1/2 MAPK Signalweg reguliert, welcher bekanntlich zu Zellproliferation führt. Unsere Studie hebt die Bedeutung von ANGPTL4 als ein essentieller Regulator von Fibroblastenproliferation hervor, wodurch es zur Entstehung von Lungenfibrose kommen kann.

Abstract

Idiopathic pulmonary fibrosis (IPF) is a fatal, irreversible, and often lethal lung disease of unknown cause. The lung tissue becomes thick, stiff and scarred/fibrotic over time. The pathogenesis of IPF is not well understood. It is known that extracellular matrix (ECM) proteins are involved in the pathobiology of IPF. Angiopoietin-like 4 (Angptl4) is one of these ECM proteins and might take part in the IPF pathophysiology. Therefore, in the current study we aimed to understand the role of Angptl4 in the pathogenesis of pulmonary fibrosis. Angptl4 in IPF diseases were assessed using a combination of several *in vitro* experiments. Isolated parenchymal fibroblasts served as *in vitro* tools to decipher signaling mechanisms. We observed that the platelet-derived growth factor (PDGF-BB) leads to a time dependant increase of Angptl4 expression in human parenchymal fibroblasts. This PDGF-BB mediated Angptl4 expression is regulated trough the Ras/MEK/ERK1/2 MAPK pathway, which is known to lead to cell proliferation. Our study emphasizes the importance of Angptl4 as an essential regulator of fibroblast proliferation, which may lead to pathogenesis of pulmonary fibrosis.

1 Introduction

1.1 Interstitial lung disease

Pulmonary disorders can lead to an interstitial lung disease such as idiopathic pulmonary fibrosis (IPF). IPF is characterized by an irreversible accumulation of connective tissue in the interstitium of the lung. The lung tissue becomes thick, stiff and scarred over the time. IPF is a mostly lethal lung disease of a unknown cause [1].

1.2 Fibroblasts

Fibroblasts belong to the connective-tissue cell family and are present in every human tissue. These cells originate from mesenchymal cells [2]. Fibroblasts play a role in the synthesis of the extracellular matrix (ECM) components [3]. The major product of fibroblasts is collagen, which is responsible for the maintenance of ECM [3]. Fibroblasts are also involved in wound healing [4]. Fibroblasts can be activated to support proliferation and cell differentiation via chemical signals such as local increase of active TGF- β [1, 5-7]. This chemical stimulation leads to changes in the gene expression, and the differentiation of fibroblasts to myofibroblasts. This differentiation takes part in the inflammatory response after injury [5-7]. Fibroblasts also play a role in the majority of organ failure cases [3]. In the lung, fibroblasts are involved in the pathogenesis of IPF [1]. Hallmarks of the disease are an increased ECM accumulation and an escalated proliferation of fibroblasts [8]. Cytokines such as platelet-derived growth factor (PDGF) stimulate proliferation and lead to fibrotic response [7].

1.3 Platelet-derived growth factor and its signaling

PDGF-BB belongs to the platelet-derived growth factor family. It is a mitogen factor for connective tissue cells such as fibroblasts and smooth muscle cells [9]. PDGF plays an essential role in wound healing [10]. The PDGF family includes four cystine-knot-type growth factors (PDGF-A,-B,-C,-D). PDGF is functionally active as a dimer of two polypeptide chains, which are linked by intermolecular disulphide bonds [11-13]. There are three different dimeric forms of PDGF known (PDGF-AA, PDGF-BB and PDGF-AB) [10]. The dimeric forms of PDGF have different function. For example, PDGF-AB has a higher mitogenic function than PDGF-AA [14].

PDGF-B contains (figure 1.1) a signal peptide, following a ~60 amino acids long pro-peptide sequence and a cleaving site at the N-terminus [15]. At the C-terminus PDGF-B contains a cysteine-knot domain, which is highly conserved in all PDGFs forms and a highly polar ~30 amino acids long tail [16-18]. In the intracellular secretion pathway PDGF-B can be cleaved by proprotein convertases such as furin between the pro-peptide domain and the cysteine-knot domain [11, 19]. PDGF-B is already proteolytically processed before secretion [11].



Figure 1.1: Structure of PDGF-B. SP: signal peptide domain; PRO: pro-protein domain; RGRR: cleaving site; Cys-Knot: cysteine-knot domain [20].

In human fibroblasts PDGF-BB binds to the PDGF receptor α and PDGF receptor β . However, PDGF-BB binds with higher affinity to PDGF receptor β . Both PDGF receptors are tyrosine kinases [21-23]. The PDGF receptors have an extracellular immunoglobulin (IG)-like domain, a transmembrane domain and an intracellular kinase domain [24, 25]. The active PDGF-BB interacts with the extracellular Ig-like domain of two PDGF receptor molecules and builds a ligand receptor complex with them [26]. This interaction leads to a change in the conformation of the PDGF receptor, which brings the kinase domains together [27]. The kinase domain carries two major auto-phosphorylation sites which initiate the downstream signaling (figure 1.2) [28]. This process leads to a signal cascade, which activates transcription factors for the regulation of cell growth and survival such as activator protein 1 (AP-1) [29, 30]. PDGF-BB can lead through the activation of Ras/MEK/ERK1/2 MAPK signaling pathways to cell proliferation [31, 32]. This PDGF signaling induced proliferation may also be involved in the pathogenesis of pulmonary fibrosis. Fibrotic tissue in general is characterized by excessive deposition of ECM, which leads to an increase of PDGF activation [33]. The mechanisms that mediate increased PDGF activation in the process of pulmonary fibrosis are not well understood. In pulmonary fibrosis the signaling of both PDGF receptors (α/β) have assigned roles [34]. The PDGF receptor β is involved in mediating fibroproliferative responses [34, 35].

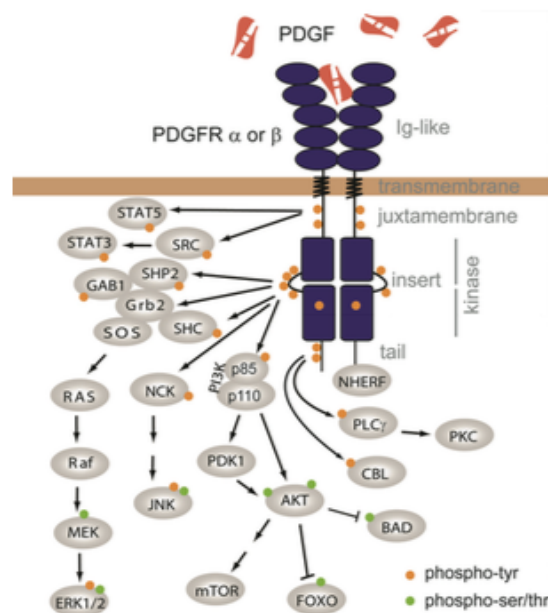


Figure 1.2: Signaling of PDGF. PDGF receptors domains and binding of PDGF to the receptor. Arrows show different PDGF induced pathways. The orange points show tyrosin phosphorylation and the green points serin/tyrosin phosphorylation [11]

1.4 Angiopoietin-like 4

ECM proteins have been implicated in the pathobiology of IPF and Angiopoietin-like 4 (Angptl4) has been described as a component of ECM. Angptl4 belongs to the ANGPTL (Angiopoietin-like) family (Angptl1-7) and is a secreted protein. ANGPTL family members are found in human and mice, expect for Angptl5, which is only expressed in human [36]. Hence, Angptl4 gene is well conserved in different species. The gene is localized on chromosome 19p13.3. and encodes a 406 amino acid glycoprotein [36].

Members of the ANGPTL family are primarily involved in regulation of angiogenesis and have a high similarity to the angiopoietin family [37]. Angptl3, Angptl4 and Angptl6 also play a role in the regulation of lipid metabolism [38].

Angptl4 is expressed in many different tissues. It is primarily expressed in adipose tissue [39] with more moderate expression in liver [37], heart [40], skeletal muscles, kidney [41], intestine [42], brain, thyroid [43] as well as in pituitary gland, spleen [44], hypothalamus [45], placenta [46-48]

and lung [49]. Angptl4 is a target of peroxisome proliferation activators (PPARs) (51, 52) and its expression is upregulated under ischemic and hypoxic conditions (53).

1.4.1 Structure of Angiopoietin-like 4

Angptl4 has a molecular mass of approximately 65kDa and contains a secretory signal peptide, an N-terminal coiled-coil domain, a linker region and a large C-terminal fibrinogen-like domain, which is well conserved in the ANGPTL family (figure 1.3) [36]. It has three potential N-glycosylation sites [36]. The full-length Angptl4 can be proteolytically cleaved by proprotein convertases at the linker region to generate an N-terminal coiled-coil domain and a C-terminal fibrinogen-like domain [50]. The N-terminal coiled-coil domain has a molecular mass of 15-26kDa and is involved in lipid metabolism [51-53]. The C-terminal fibrinogen-like domain has a molecular mass of 37-47kDa and interacts with integrins β 1 and β 5 and their ECM proteins [54, 55]. The highly hydrophobic signal peptide is important for the secretory pathway [50]. The cleavage seems to be tissue dependent. For example, the adipose tissue only secretes the full-length Angptl4 and the liver only the N-terminal coiled-coil domain in human [56]. After the cleavage the N-terminal coiled-coil domain circulates as an oligomer and the C-terminal fibrinogen-like domain as a monomer [51]. Via intermolecular disulfide bonds the native full-length Angptl4 may form higher-order structures [53].

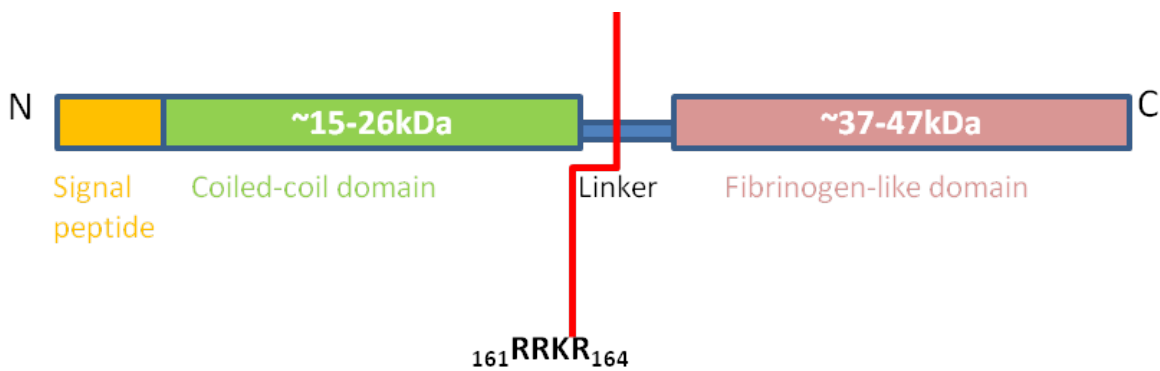


Figure 1.3: Structure of Angptl4. Angptl4 can be proteolytically cleaved at the linker region (RRKR) into an N-terminal coiled-coil domain (15-26kDa) and a C-terminal fibrinogen-like domain (37-47kDa).

1.4.2 Function of Angiopoietin-like 4

Angptl4 is a component of the ECM and coordinates the cell-matrix communication [55]. The best investigated function of Angptl4 is the one as an important regulator of glucose homeostasis, insulin sensitivity and lipid metabolism [51, 57-59]. The two domains of ANGPTL4 have different functions. The N-terminal coiled-coil domain leads to inhibition of lipoprotein lipase (LPL) by disruption of the dimerization of LPL [58]. Monomeric LPL is not stable and cannot hydrolyse plasma triglycerides, leading to higher release of fatty acid [58]. The C-terminal fibrinogen-like domain can interact with the integrins $\beta 1$ and $\beta 5$ and their ECM proteins [54, 55] and seems to play a role in inhibition of angiogenesis [26]. However, many functions of Angptl4 are still unknown.

1.4.3 Angiopoietin-like 4 in disease

Angptl4 is almost ubiquitously expressed in humans and is involved in many pathophysiological processes (figure 1.4) [60].

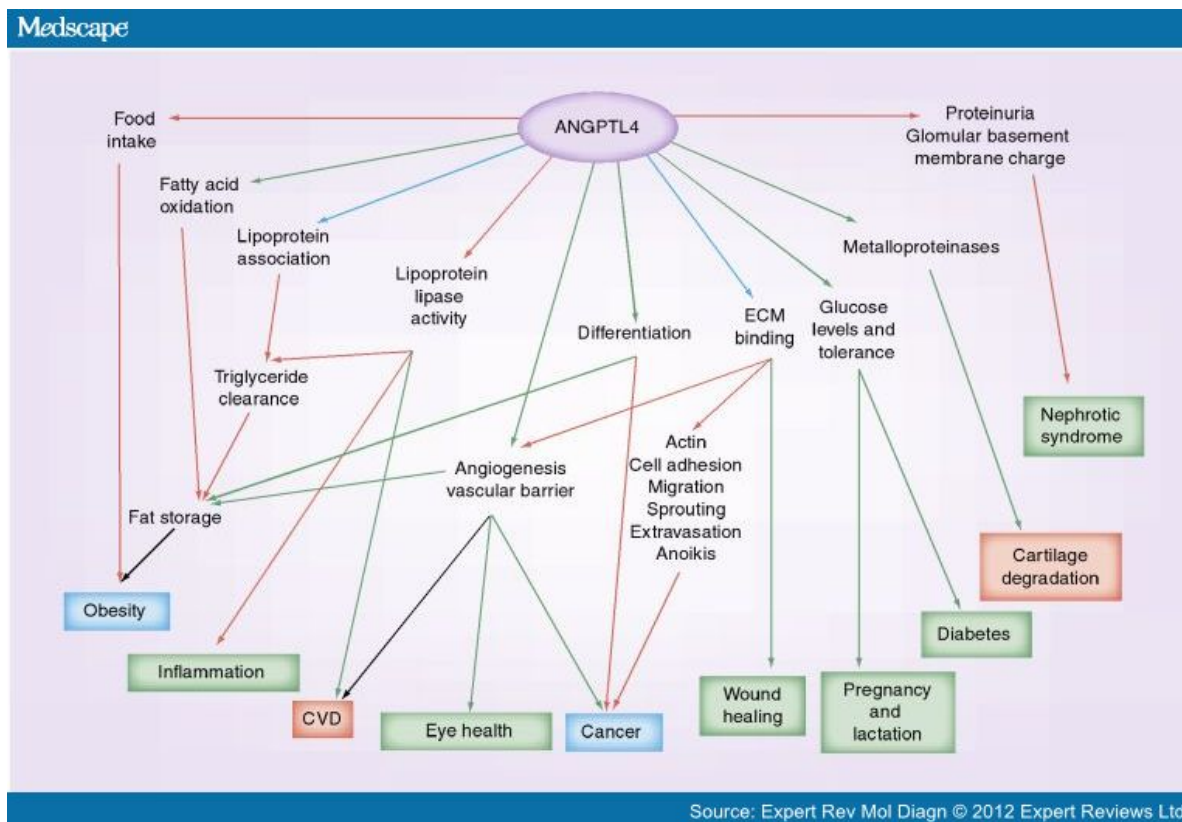


Figure 1.4: An overview of pathophysiological mechanisms in which Angptl4 plays a role. Green arrows=increase of the effect; red arrows=decrease of the effect; black arrows=increase/decrease of the effect; CVD= Cardiovascular disease [60].

For example, Angptl4 plays a role in wound healing by interacting with vitronectin and fibronectin and delays the degradation of the ECM-proteins by proteases [54, 55]. During the remodelling phase of wound healing Angptl4 regulates the protein kinase C (PKC) and the transcription factor activator protein 1 (AP-1) [61]. Thus, Angptl4 leads to increased expression of cJun and JunB. This is important for the maturation of the epidermis during the wound healing [61] (figure 1.5). So far there is nothing known about the role of Angptl4 in PDGF-BB mediated proliferation of human parenchymal fibroblasts.

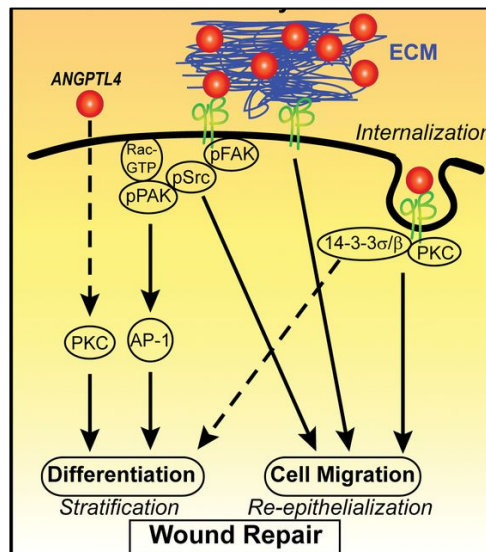


Figure 1.5: Mechanism of Angptl4 in tissue remodelling [62].

2 Aim of the study

In this study we aimed to investigate the role of Angptl4 in PDGF-BB induced proliferation of human parenchymal fibroblasts. We hypothesized (figure 2.1) that PDGF-BB elevates Angptl4 expression via AP-1 complex (Fra1/2, c-fos, fosB, c-Jun, JunB), which leads to an increase of proliferation of human parenchymal fibroblasts. Furthermore, we hypothesized that Angptl4 is secreted by human parenchymal fibroblasts.

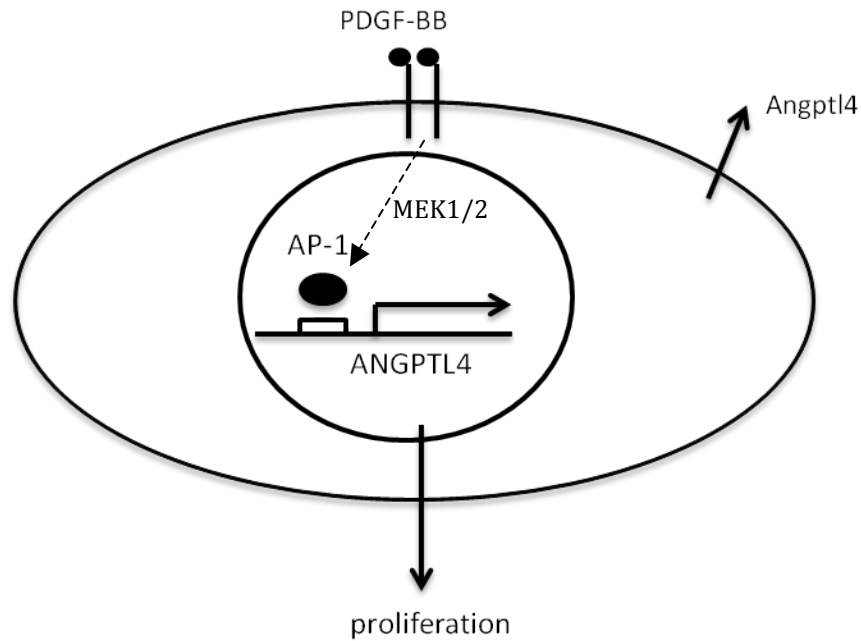


Figure 2.1: Schematic representation of possible Angptl4 regulation in human parenchymal fibroblasts.

3 Material and Methods

3.1 Cell culture

3.1.1 Primary cells in cell culture

Human lungs samples were received from the Medical University of Vienna (Department of Surgery, Deivision of Thoracic Surgery, Vienna, Austria) and the application were approved by the institutional ethics commission (EK976/2010) of Vienna and patient consent was obtained before lung transplantation.

Human primary parenchymal fibroblasts were isolated from these lungs in our labortory. Fibroblats were cultured in full DMEM/F-12 medium (Gibco, Life Technologies). The human parenchymal fibroblasts were kept in incubator (Binder, Tuttlingen, Germany) at 37°C and 5% CO₂. All cells were used between passages 1-7.

Table 1: Media used for cell culture.

Media	Components	Company
Full DMEM/F-12 Medium	10% FCS 1% Glutamin 0.2% antibiotics	Gibco, Life Technologies
Basal DMEM/F-12 Medium	0% FCS 0% Glutamin 0.2% antibiotics	Gibco, Life Technologies

3.1.2 Transfection of primary cells

For the silencing of Angptl4, human parenchymal fibroblasts were seeded in 6 well plates (150,000 cells/well). The day after, 2 hours (h) before transfection, the medium was changed to basal medium (Gibco, Life Technologies, CA, USA). For the transfection the Effectene Transfection Reagent (Qiagen, Hilden, Germany) was used. The siRNA (Thermo Scientific, MA, USA (table 2)) and the siControl (Thermo Scientific, D-001810-10-05, MA, USA) were applied at a concentration of 25 nM. First the siRNA, the DNA-condensation buffer (Buffer EC) and the Enhancer were mixed. Afterwards the mixture was vortexed for 1 second (sec) and incubated at room temperature (RT) for 5 minutes (min) This first step leads to DNA condensation by interaction with the Enhancer in the Buffer EC.

Effectene (Qiagen, Hilden, Germany) was added to the condensed DNA and the mixture was vortexed for 10 sec and incubated at RT for 10 min. The basal medium was added and the mixture was pipetted onto the cells. After 6 h the medium was changed to full medium. After 48 h of silencing the cells were stimulated with platelet derived growth factor for 30 min, 1 h, 3 h, 6 h, and 24 h.

Table 2: siRNA used for transfection of primary cells.

Target gene	Target sequence	Company	Product number
ANGPTL4	GAUGGAGGCUGGACAGUAA CCACUUGGGACCAGGAUCA GAAAGAGGCUGCCCGAGAU GGCAGAAGCUUAAGAAGGG	Thermo Scientific (Dharmacon)	L-007807-00-0005
jun-B	GGACACGCCUUCUGAACGU CAUACACAGCUACGGGAUA GAACAGCCCUUCUACCAG GAGCUGGAACGCCUGAUUG	Thermo Scientific (Dharmacon)	L-003900-00-0005
c-jun	GAGCGGACCUUAUGGCUAC GAACAGGUGGCACAGCUUA GAAACGACCUUCUAUGACG UGAAAGCUCAGAACUCGGA	Thermo Scientific (Dharmacon)	L-003268-00-0005
c-fos	GGGAUAGCCUCUCUACUA ACAGUUAUCUCCAGAAGAA GAACCGUCAAGAGCAUCA GCAAUGAGCCUCCUCUGA	Thermo Scientific (Dharmacon)	L-003265-00-0005
fra-2	GGCCCAGUGUGCAAGAUUA CAGAAAUUCCGGGUAGAU CCACUCUGCUGGCUCUGUA ACACAUGGCCCUCCCAAGA	Thermo Scientific (Dharmacon)	L-004110-00-0005

3.1.3 Stimulation of primary cells

To investigate which kinases are involved in Angptl4 regulation upon PDGF-BB stimulation different inhibitors (table 3) were applied. For this experimental set-up 150,000 human parenchymal fibroblasts per well were seeded in 6 well plates. On the next day, the medium was changed to basal medium overnight. For the inhibition of specific kinases, 1 h before stimulation with PDGF-BB, the inhibitors/DMSO (table 3) were added to the cells. For the stimulation 10 ng/ml of the PDGF-BB was applied. The cells were harvested after 6 h stimulation time and the supernatants were collected.

Table 3: Inhibitors utilized for cell stimulation.

Inhibitors	Concentration (start)	Concentration (final)	Company
SB203580 (p38)	8 mM	8 μ M	Sigma Aldrich
SP600125 (JNK)	90 mM	5 μ M	Sigma Aldrich
U0126 (MEK1/2)	10 mM	50 μ M	Sigma Aldrich
Wortmannin (PI3K/Akt)	8 mM	80 μ M	Sigma Aldrich

3.1.4 Proliferation assay

To investigate the effect of Angptl4 on the proliferation of human parenchymal fibroblasts, Angptl4 was silenced and cells were subsequently stimulated with PDGF-BB. First 150,000 cells/well were seeded in 6 well plates. The day after, 2 h before transfection, the medium was changed to basal medium. The cells were transfected as described in section 3.1.2. On the next day, the cells were trypsinized (Trypsin, Gibco, Life Technologies, CA, USA). Afterwards 10,000 cells/well were seeded in 96 well plates. After 8 h the medium was changed to basal medium. After 12 h the basal medium was changed and the cells were stimulated with 10 ng/ml PDGF-BB for 24 h plus 1 μ Curie/ml of radioactive labeled [3H]-thymidine (BIOTREND Chemikalien GmbH). For the control 1 μ Curie/ml of radioactive labeled [3H]-thymidine was added to the basal medium. The cells were harvested after 24 h. Afterwards the cells were dried for 2 h and 25 μ l of scintillation cocktail was added to the cells. The amount of cells was read by a scintillation counter (Wallac 1450 MicroBeta TriLux Liquid Scintillation Counter & Luminometer). The radioactive experiments were performed Valentina Biasin, PhD.

3.2 Molecular biology techniques

3.2.1 Isolation of RNA

For the RNA isolation of the human parenchymal fibroblasts the peqGOLD Total RNA Kit (PeqLab, Erlangen, Germany) was utilized. The RNA was isolated with 300 μ l of the RNA Lysis Buffer T from the 6 well plates. The same volume of 70% ethanol was added to the the cell lysat and subsequently mixed by vortexing. The mixture was loaded to a PerfectBind RNA Column and centrifuged for 1 min at 10.000xg. This step is necessary to bind the RNA on the PerfectBind RNA Column. Then the RNA was washed with 500 μ l RNA Wash Buffer I and centrifuged for 15 seco at 10.000xg. Afterwards the mixture was washed two times with 600 μ l RNA Wash Buffer II and centrifuged for 15 sec at 10.000xg each time. After washing the column was dried by centrifugation for 2 min at 10.000xg. Finally the RNA was eluted with 30 μ l sterile RNase-free dH₂O. RNA isolation was done according to the manufacturer's protocol. After RNA isolation the concentration of the RNA was measured at 260 nm with the Nanodrop spectrophotometer (Rockland, IL).

3.2.2 cDNA synthesis

For the cDNA synthesis the iScript kit (BioRad, Hercules, CA, USA) was used to reverse transcribe the isolated RNA into cDNA. The components were mixed to a total volume of 20 μ l (table 4) according to the manual and the PCR was run according to the reaction protocol (table 5). The final concentration of the constructed cDNA was 50 ng/ μ l.

Table 4: Components and volumes used for the iScript cDNA synthesis.

Components	Volume/reaction
5x iScript reaction mix	4 μ l
iScript reverse transcriptase	1 μ l
Nuclease-free water	x μ l
RNA template (1000 ng)	x μ l
Total volume	20 μ l

Table 5: PCR reaction protocol for iScript cDNA synthesis.

iScript cDNA Synthesis Reaction Protocol	
25°C	5 min
42°C	30 min
85°C	5 min
4°C	Hold at

3.2.3 Real-time-PCR

The cDNA from section 3.2.2 was applied for the Real-time PCR. The cDNA was diluted 1:10 with RNase-free water. For the Real-time PCR the QuantiFast® SYBR® Green PCR kit (Qiagen, Hilden, Germany) was employed. The QuantiFast® SYBR® Green PCR Master Mix includes the following components: HotStarTaq Plus DNA Polymerase, QuantiFast® SYBR®Green PCR Buffer, SYBR® Green and ROX passive reference dye. A MasterMix, which included 5 µl of QuantiFast® SYBR®Green PCR Master Mix and 1 µl of the Primer (including reverse primer and forward primer)(table 6) was prepared for duplicates. Then 6 µl of the MasterMix were mixed with 4 µl of 1:10 diluted cDNA sample and two times 4 µl of the mixture were pipetted in one well each of a 384 well plate (Roche, Rotkreuz, CH). To limit the pipetting mistakes duplicates were done. As a reference gene beta-2-microglobulin (B2M) and porphobilinogen deaminase (PBGD) were used (table 6). The Real-time PCR was run in a LightCycler 480 (Roche, Rotkreuz, CH).

Table 6: Primer sequences.

Primer	Species	Access. No.	Forward primer (5' - 3')	Reverse primer (5' - 3')
Angptl4	human	NM_001039667.1	GGCCAAGCCTGCCCCGAAG AA	CAGCCAGAACTCGCCGT GGG
B2M	human	NM_004048.2	CCTGGAGGCTATCCAGCG TACTCC	TGTCGGATGGATGAAAC CCAGACA
PBGD	human	NM_000190.3	TCGGAGCCATCTGCAAGC GG	GCCGGGTGTTGAGGTTT CCCC

The Real-time PCR reactions were run with the following protocol:

Table 7: The Real-time PCR temperature program.

Real-time PCR temperature program			
	95°C	5 min	
Denaturation	95°C	5 s	45 cycles
Annealing	60°C	5 s	
Extension	72°C	10s	

To analyse the Real-time PCR results the quality of the duplicates was checked at first. Therefore the melting curve of the amplified PCR product was confirmed. One peak means that the binding of SYBR® Green to the double strand DNA is specific. An unspecific binding is indicated by two peaks. Then the averages of the duplicates from the reference genes and the genes of interest were calculated. Following the ΔC_t was calculated: C_t reference gene - C_t gene of interest. To minimize the statistical variance in the groups the $\Delta\Delta C_t$ was calculated: ΔC_t gene of interest - ΔC_t control. The $\Delta\Delta C_t$ values were shown as a graph by using the software GraphPad Prism 5 (GraphPad Software, CA, USA).

3.2.4 Protein isolation

For the protein isolation 300 μ l of cold Radio- Immunoprecipitation Assay Buffer (RIPA) (Sigma-Aldrich, MO, USA, (table 8)) supplemented with protease and phosphatase inhibitors (Thermo Scientific, MA, USA) was put in each well of the plates. The cells were scratched from the plates via Corning® Costar 3010 Cell Scraper (Corning®, NY, USA).

3.2.5 SDS-Page and western blot

For the SDS-Page 10 % SDS polyacrylamide gels were used (table 8). The protein samples were thawed on ice and centrifuged for 2 min at 4°C. The supernatant was pipetted into a new tube. 10X SDS sample Buffer (table 9) was added to the supernatant. Afterwards the samples were cooked in a Thermomix (Eppendorf, Hamburg, Germany) at 95°C for 10 min.

As a molecular mass control (from 10 kDa to 250 kDa), the Precision Plus Protein Standard (BioRad, CA, USA) was used. The gel electrophoresis (PowerPac™ Basic Power Supply, BioRad, CA, USA) was run at 120V for 2 h. Afterwards the proteins were blotted from the gel onto a polyvinylidene difluoride (PVDF) blotting membrane (GE Healthcare Life Science, WI, USA) by using the PowerPac™ Basic Power Supply (BioRad, CA, USA) filled up with 1% Transfer buffer at 120V for 1 h and 30 min at 4°C. The membrane was blocked with 1% non-fat dry milk (Carl Roth GmbH, Karlsruhe, Germany) in TBS-T (1xTBS + 0,1% tween 20) buffer (table 9) for 1 h at RT. Finally the membrane was incubated with the primary antibody (table 10) over night at 4°C. The next day the membrane was washed 3x for 5 min with TBS-T and afterwards incubated with the secondary antibody (α -rabbit IgG;HRP-linked Antibody, Cell Signaling Technology, MA, USA) diluted 1:5000 in 1% non-fat dry milk for 1 h at RT. Then the membrane was washed for 4x 15 min with TBS-T. For the detection 1 ml of ECL solution (Prime Kit, Amersham Biosciences, Freiburg, Germany) was used and incubated for 5 min on the membrane. For the Chemiluminescence detection Kodak films (GE Healthcare Life Science, WI, USA) were used and developed via AGFA Curix 60 Fim Processor (AGFA Health Care, SC, USA). After detection the membrane was stripped with Resore™ PLUS Western Blot Stripping Buffer (Thermo Scientific, MA, USA) for 15 min at RT and was washed for 3x 5 min with TBS-T. The membrane was then blocked with 1% non-fat dry milk in TBS-T for 1 h at RT and incubated with α -Tubulin antibody (table 10), to check if the protein loading was equal. All buffers were prepared as described in table 9.

Table 8: Compounds to produce one 10% SDS polyacrylamide gels.

Separation gel	
ddH ₂ O	3.2 ml
30% Acrylamid	2.67 ml
1.5M Tris pH 8.8	2 ml
10% SDS	80 µl
10% APS	80 µl
TEMED	8 µl
Total volume	8 ml
Stacking gel	
ddH ₂ O	2.6 ml
30% Acrylamid	1 ml
0.5M Tris pH 6.8	1.25 ml
10% SDS	50 µl
10% APS	50 µl
TEMED	5 µl
Total volume	5 ml

Table 9: Buffers used for SDS-Page and western blot.

Buffer	Compounds	Company
RIPA Buffer	150 mM NaCl 1.0% IGEPAL® CA-630 0.5% Sodium Deoxycholate 0.1% SDS 50 mM Tris pH 8.0 storage at 4°C	Sigma- Aldrich
30% Acrylamid	storage at 4°C	Merck KGaA
1.5M Tris	1.5 M Tris pH 8.8	
0.5M Tris	0.5 M Tris pH 6.8	
10% SDS	50 g Na Serva 20783 500 g dH ₂ O	Pharmacy LKH Univ. Klinikum Graz
10% APS	1 g Ammonium persulfate 10 ml dH ₂ O	
TEMED	storage at 4°C	Sigma- Aldrich
10x SDS Sample Buffer	500mM Tris 20% SDS 50% Glycerol 0.2% Bromophenol Blue 50 µl β-Mercaptoethanol	

10x Running Buffer	30 g/l Tris 144 g/l Glycin 10 g/l SDS fill-up with 1l dH ₂ O pH 8.6	
10x Transfer Buffer	28 g/l Tris 143 g/l Glycerin fill-up with 1l dH ₂ O	
1x Transfer Buffer	100 ml 10x Transfer Buffer 200 ml MetOH 700 ml dH ₂ O for 1l storage at 4°C	
10x TBS	24,2g TRIS Base (20mM) 80g NaCl (137mM) fill-up with 1l dH ₂ O pH 7.6	

Table 10: Antibodies for western blot.

Antibody	Source	Dilution	Company	Product Nr
hANGPTL4	rabbit	1:1000	BioVendor	# RD181073100-01
α-tubulin	rabbit	1:5000	Cell Signaling Technology	# 2125

3.2.6 Coomassie blue staining

As a loading control for the collected cell supernatant (section 3.1.3), the SDS polyacrylamide gel was stained with Coomassie Blue Solution (table 11). After the gel electrophoresis was run (section 3.2.5) the gel was stained with Coomassie Blue until the gel was blue. Then the blue stained gel was destained.

Table 11 Solutions used for Coomassie Blue staining.

Solution	Compounds	Company
Coomassie Blue Solution	0.1 g Coomassie Brilliant Blue G-250	BioRad
	50 ml MetOH	MerckMillipore
	20 ml Acetic Acid	MerckMillipore
	30 ml dH ₂ O	
Destaining Solution	300 ml MetOH	MerckMillipore
	100 ml Acetic Acid	MerckMillipore
	700 ml dH ₂ O	

3.3 Cloning

3.3.1 Media

All media were prepared as described in table 12. The media were autoclaved for 20 min at 121°C. Glucose (Sigma- Aldrich, MO, USA) was added after autoclaving. The Ampicillin (50 mg/ml in H₂O, Sigma- Aldrich, MO, USA) working concentration for the LB-medium and LB-plates was 20 µg/ml.

Table 12: Media used for cloning.

Media	Components	Concentration
LB	Tryptone	10 g/l
	yeast extract	5 g/l
	NaCl	10 g/l
LB plates	+Bacto-agar	15 g/l
SOC medium	Tryptone	10 g/l
	yeast extract	5 g/l
	NaCl	0.5 g/l
	KCl	250 mM
	Glucose	20 mM

3.3.2 Template cDNA

To establish a template cDNA (cJun), isolated RNA (section 3.2.1), from human donor parenchymal fibroblasts was used. The template cDNA was synthesized with the RevertAid First Strand cDNA Synthesis kit (Thermo Scientific, MA, USA) according to the manufacturer's protocol (table 13, table 14).

Table 13: Components used for the RevertAid First Strand cDNA Synthesis.

Template RNA	Total RNA	5 µl (0.1 ng-5 µg)
Primer	Oligo (dT) ₁₈ primer	1 µl
Nuclease-free Water		6 µl
Total volume		12 µl

Table 14: PCR temperature program.

cDNA Synthesis PCR temperature program			
	94°C	3 min	
Denaturation	94°C	30 s	35 cycles
Annealing	58°C	30 s	
Extension	72°C	45 s	

3.3.3 Establishment of the cJun-fragment

The AmpliTaq Gold® 360 Master Mix (Applied Biosystems, CA, USA) was applied to produce the cJun-fragment (figure 3.1). To optimize the PCR reaction a gradient PCR with different annealing temperatures (C:71°C, D:67.2°C, E:62.5°C, F:58.9°C, G:56.5°C) was performed. The gradient PCR was performed according to the manufacturer's protocol (table 15, table 16). Primers used are listed in table 17. The size of the c-Jun fragment was 1000bp long, therefore the elongation time was calculated with 1 min. gradient PCR products were analyzed and separated on a 1.2% agarose gel described in section 3.3.4. Afterwards the PCR was run again with the before optimized annealing temperature 56.5°C to establish the cJun-fragment.

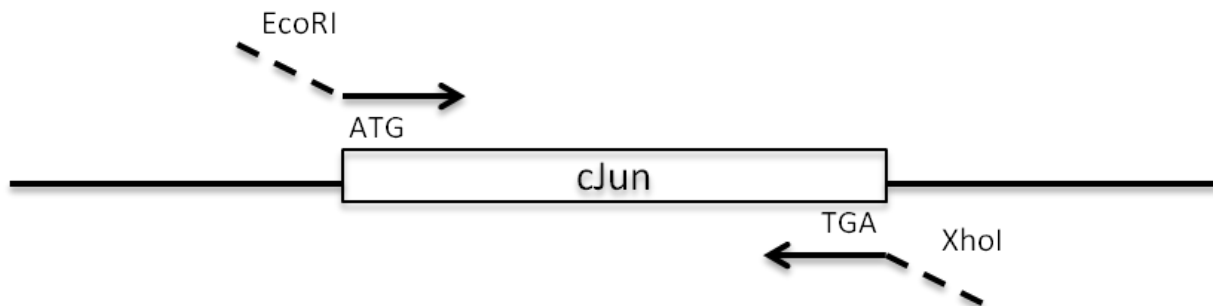


Figure 3.1: The designed primers, which were used for the gradient PCR. The primers bind to the cDNA with the 20bp cJun sequence and generate the cJun fragment with the restriction sequence (EcoRI, XhoI) on each end.

Table 15: Components used for the AmpliTaq Gold® 360 Master Mix PCR reaction.

Component	Volume per 25 µl reaction
360 GC Enhancer	2.5 µl
AmpliTaq Gold®360 Master Mix	12.5 µl
h_EcoRIcjun_fw	1 µl
h_XhoIcjun_rv	1 µl
cDNA	2 µl
RNase-free Water	6 µl
Total PCR volume	25 µl

Table 16: PCR temperature program for the gradient PCR.

Gradient PCR temperature program			
		95°C	5 min
Denaturation	95°C	30 s	40 cycles
Annealing	T _{A(C-G)}	30 s	
Extension	72°C	1 min	
		72°C	10 min
T _A : C 71°C, D 67.2°C, E 62.5°C, F 58.9°C, G 56.5°C			

Table 17: Primer sequences utilized for the establishment of the cJun fragment. The highlighted letters are the recognition sites for the restriction enzymes EcoRI and XhoI.

Oligoname	Sequence	Product
h_EcoRIcjun_fw	5'..ATTAGAA TTCTGACGGACTGTTCTATGACTGC ..3'	
h_XhoIcjun_rv	5'..ATTACT CGAGTT CAAAATGTTTGCAACTG..3'	~1kb

3.3.4 Electrophoresis

The PCR products were separated on a 1.2% agarose gels with 7 μ l PeqGreen in 1X TAE Buffer (table 18) at 95V. Under UV light the PCR cDNA fragments were visualised.

Table 18: Buffer used for the gel electrophoresis.

Buffer	Components	Company
50X TAE Buffer	242g/l TrisBase 57.1ml acetic acid 100ml 0.5M EDTA pH 8.0	Sigma Aldrich

3.3.5 Purification of PCR products

The PCR product from section 3.3.3 (cJun) was purified with peqGOLD Cycle-Pure Kit (PEQLAB, Erlangen, Germany) according to the manufacturer's protocol. This step is necessary to remove salt, free nucleotides, oligonucleotides, polymerases and enzymes. The PCR product was mixed with the same volume of CP Buffer (a special Binding Buffer) by vortexing thoroughly. The mixture was loaded onto a PerfectBind DNA Column and the mixture was centrifuged for 1 min at 10.000xg. The DNA binds to the PerfectBind DNA Column and the Column was washed two times with 750 μ l CG Wash Buffer and was centrifuged each time for 1 min at 10.000xg. Then the column was dried by centrifugation for 1 min at 10.000xg. The DNA was eluted with 30 μ l dH₂O.

3.3.6 Restriction

Purified PCR product (cJun) and a plasmid (pcDNA3.1 (+)) (supplement figure 6.1) were cut with the restriction enzyme EcoRI and XhoI (both from New England BioLab®, MA, USA) (table 19). The restriction samples were prepared as described in table 20 and were incubated in Thermomix (Eppendorf, Hamburg, Germany) at 37°C for 1.5 h. In the 10x NEBuffer 3 (New England BioLab®, MA, USA) the activity of XhoI was 100%. The double amount of EcoRI was used, as its activity was only 50% in 10x NEBuffer 3. Afterwards the restriction samples were separated on a 1.2% agarose gel (details in section 3.3.4), and the bands were isolated from the gel and eluted.

Table 19: Restriction enzymes utilized for cutting the cJun fragment and plasmid (pcDNA3.1 (+)).

EcoRI	5'...GATATC...3' 3'...CTATAG...5'
XhoI	5'...CTCGAG...3' 3'...GAGCTC...5'

Table 20: Components for the restriction reaction.

Plasmid (pcDNA3.1 (+)) (1µg)	1 µl	Insert (cJun)	15 µl
10x NEBuffer 3	2 µl	10x NEBuffer 3	2 µl
XhoI (1U/ml)	0.2 µl	XhoI (1U/ml)	0.2 µl
EcoRI (1U/ml)	0.4 µl	EcoRI (1U/ml)	0.4 µl
H ₂ O (Millipore)	16.4 µl	H ₂ O (Millipore)	2.4 µl
Total volume	20 µl	Total volume	20 µl

3.3.7 Gel Extraction

The restriction products from section 3.3.6 were eluted with QIAEX II Gel Extraction Kit (QIAGEN, CA, USA) according to the manufacturer's protocol. The QIAEX II Gel Extraction Kit purifies 40bp to 50kb DNA fragments from agarose gel. The DNA bands were excised from the agarose gel and gel slices were weighted. Afterwards the Buffer QX1 was added to the gel slices in a ratio of three to one. The agarose gel was solubilized and bound to the QIAEX II silica particles by Buffer QX1. For the optimal DNA binding a pH \leq 7.5 is required. Hence Buffer QX1 contained a pH indicator. The mixture was vortexed and incubated in a Thermomix (Eppendorf, Hamburg, Germany) at 50 °C for 10 min (every 2 min vortexing the mixture). This step is necessary to solubilize the agarose gel and bind the DNA. Afterwards the mixture was centrifuged for 30 sec and the supernatant was removed. The pellet was washed once with 500 µl of Buffer QX 1, two times with 500 µl of Buffer PE and following air-dry the pellet. The pellet was resolved in 20 µl dH₂O and incubated at RT for 5 min. After centrifugation for 30 seconds the supernatant including DNA was transferred into a clean tube. The DNA concentration was measured with the Nanodrop (Rockland, IL).

3.3.8 Ligation

Afterwards the extracted DNA samples were ligated. For the ligation the T4 Ligase and the T4 buffer (both from New England BioLab®, MA, USA) were applied. The plasmid (pcDNA3.1 (+)) and the insert (cJun) proportion was 1:3 in the ligation preparation (table 21). The ligation samples and control were incubated in a Thermomix (Eppendorf, Hamburg, Germany) at 16°C for 3 h.

Table 21: Components for the plasmid and insert ligation.

Plasmid + Insert (1:3)		Control (plasmid without insert)	
T4 buffer	2 µl	T4 buffer	2 µl
T4 ligase	1 µl	T4 ligase	1 µl
Plasmid (pcDNA3.1 (+))	5 µl	Plasmid (pcDNA3.1 (+))	5 µl
Insert (cJun)	2 µl	Insert (cJun)	-
H ₂ O (millipore)	10 µl	H ₂ O (millipore)	12 µl
Total volume	20 µl	Total volume	20 µl

3.3.9 Transformation

The constructs (pGEMT-hu-JunB, CMV-hu-Fra-2 [pcDNA3]) were obtained from Latifa Bakiri Ph.D (Genes, Development and Disease Group headed by Prof. Erwin Wagner, Spanish National Cancer Research Center Genes, Spain). The maps of the two plasmids are shown in the supplement (figure 6.1, figure 6.2).

Table 22: Vectors used for the transformation in *E.coli*.

Vector	Concentration of the solute vectors
pGEMT-hu-JunB	26 ng/µl
CMV-hu-Fra-2 [pcDNA3]	442 ng/µl
CMV-hu-cJun [pcDNA3.1]	Not measured

All three vectors (table 22) were transformed into the NEB5- α competent *E.coli* cells (High Efficiency C2987H (New England BioLab®, MA, USA)). The competent *E.coli* cells were thawed on ice. Then 100 ng of plasmid DNA was added to the competent cells and mixed carefully (no vortexing) as the competent cells are very sensitive. Cells were incubated on ice for 30 min. Afterwards the cells were heat shocked at 42°C for 30 sec and following kept on ice for 5 min. Then 950 μ l SOC Medium (New England BioLabs®, MA, USA, (table 12) was added and carefully shook by Thermomix (Eppendorf, Hamburg, Germany) at 37°C for 60 min. Then the cells were diluted in SOC medium (1:1, 1:10, 1:100) and the dilutions were spread (100 μ l) onto pre-warmed (37°C) LB-plates. The plates were incubated over night at 37°C.

3.3.10 Overnight culture

For the overnight culture (ONC) two colonies were picked from section 3.3.9. Each colony was transferred into 5 ml pre warmed LB. The ONCs were grown over night at 37°C in a shaker.

3.3.11 Miniprep

The bacteria plasmids of the ONC from section 3.3.10, were isolated via QIAprep Spin Miniprep Kit (QIAGEN, CA, USA) according to the manufacturer's protocol. The bacterial cells from the ONC were centrifuged and the supernatant was removed. The pellet was resuspended in 250 μ l Buffer P1 (with RNase A) and the mixture was transferred into a new tube. Afterwards 250 μ l of Buffer P2 was added and the tubes were thoroughly mixed. Then 350 μ l of Buffer N3 was added and mixed by inverting the tube. Following the mixture was centrifuged for 10 min at 17900xg. After centrifugation 800 μ l of the supernatant was transferred to the QIAprep 2.0 spin column and again centrifuged for 1 min. The column was washed first with 500 μ l of Buffer PB (centrifuging 1 min) and then with 750 μ l of Buffer PE. Finally the column was centrifuged for 1 min to remove all wash buffer. The DNA was eluted by incubation of 50 μ l dH₂O on the column following centrifugation for 1 min. Plasmid concentrations were measured with the Nanodrop Spectrophotometer (Rockland, IL).

3.3.12 Restriction

In order to check whether the plasmid included the desired insert restriction analysis was performed. Hence the plasmid pGEMT-hu-JunB was cut with the restriction enzyme BsaHI (New England BioLab®, MA, USA) and the plasmid CMV-hu-Fra-2 [pcDNA3] with the restriction enzyme

AvaII (New England BioLab®, MA, USA (table 23)). Both restriction enzymes had 100% activity in 10x NEBuffer 4 (New England BioLab®, MA, USA). The restriction preparations were incubated in Thermomix (Eppendorf, Hamburg, Germany) at 37°C for 1.5 h (table24). Afterwards the restriction samples were separated on a 1.2% agarose gel like in section 3.3.4.

Table 23: Restriction enzymes used for the restriction reaction. Y: C or T; R: A or G; W: A or T.

BsaHI	5'...GRCGYC...3' 3'...CYGCRG...5'
AvaII	5'...GGWCC...3' 3'...CCWGG...5'

Table 24: Components used for the restriction reaction.

pGEMT-hu-JunB		CMV-hu-Fra-2 [pcDNA3]	
DNA (1µg)	1 µl	DNA (1µg)	1 µl
10x NEBuffer 4	2 µl	10x NEBuffer 4	2 µl
BsaHI (1U/ml)	0.2 µl	AvaII (1U/ml)	0.2 µl
H ₂ O (millipore)	17 µl	H ₂ O (millipore)	17 µl
Total volume	20 µl	Total volume	20 µl

3.3.13 Maxiprep

For the Maxiprep ONCs (for each Vector) with a total volume of 50 ml were used (see section 3.3.10).

The Maxiprep was performed with the EndoFree Plasmid Maxi Kit 10 (QIAGEN, CA, USA) according to the manufacturer's protocol. The bacterial pellet from the ONC was resuspended in 10 ml Buffer P1 (with RNase A). Then 10 ml of Buffer P2 were added, thoroughly mixed and the suspension was incubated for 5 min at RT. After the incubation, 10 ml of Buffer P3 was added and subsequently mixed. The solution was transferred into the barrel of the QIAfilter Cartidge (QIAGEN, CA, USA) and was incubated for 10 min at RT. Afterwards the solution was filtered into a 50 ml tube. Then 2.5 ml Buffer ER was added to the filtered lysate and incubated for 30 min on ice. The mixture was transferred to the QIAGEN-tip (QIAGEN, CA, USA), which was equilibrated before by applying 10 ml

Buffer QBT. Subsequently the solution was run by gravity flow through the QIAGEN-tip, the QIAGEN-tip was washed with 2x 30 ml Buffer QC. The DNA was eluted with 15 ml Buffer QN and the DNA was precipitated by adding 10.5 ml isopropanol (RT, Merck KGaA, Darmstadt, Germany). The lysat was mixed and centrifuged at 4°C for 30 min at 15 000xg. The supernatant was removed and the DNA pellet was washed with 5 ml of 70% ethanol (endotoxin-free, RT, Merck KGaA, Darmstadt, Germany) and centrifuged for 10 min at 15 000xg. The supernatant was again removed and the DNA pellet was air-dried. Finally the DNA was dissolved in 200 µl TE-buffer.

3.3.14 Sequencing

The sequencing of the Fra-2 and JunB inserts (supplement page 56 and 57) was performed by Eurofins Genomics (Ebersberg, Germany). The created primers are listed in table 25.

Table 25: Primer created for the sequencing of the vectors.

Primer	Sequence
JunB_fw	5'..GGACGATCTGCACAAGATG..3'
JunB_rv	5'..GTTCCCTCCTTGAAGGTGGA..3'
JunB-rv_2	5'..TGTAGGCGTCGTCGTGAT..3'
Fra-2_fw	5'..TCCCAAGACCTGGCGTGAT..3'
Fra-2_rv	5'..TCCTGTTTCACCACTACAG..3'
Fra-2_rv_2	5'..CCTCCAGCTCCTCTGTCT..3'

3.4 Statistic analysis

All statistic analyses were performed with the software GraphPad Prism 5 (GraphPad Software, CA, USA). For the statistic calculation of the Real-time PCR results and the proliferation result the one-way ANOVA, Turkey's Multiple Comparison Test or t-test was utilized. In all the results a P-value <0.05 was regarded as significant. All the results are shown as mean with standard error of the mean (SEM) (GraphPad Software, CA, USA).

4 Results

4.1 Expression of Angptl4 is elevated upon PDGF-BB stimulation in human parenchymal fibroblasts

The growth factor PDGF-BB leads to proliferation of human parenchymal fibroblasts [32]. We performed experiments to investigate if Angptl4 expression is regulated by PDGF-BB. The results show that Angptl4 expression is elevated upon PDGF-BB stimulation in a time dependent manner in human parenchymal fibroblasts (figure 4.1A). The Angptl4 expression started to increase after 1 h of PDGF-BB stimulation with the highest expression of Angptl4 after 6 h. At the later time points the Angptl4 expression was decreased again.

To investigate the expression of Angptl4 on protein level, western blots were performed (figure 4.1B). A polyclonal antibody (hANGPTL4) was applied to detect all three forms of Angptl4. The full-length form of Angptl4 was detected with a size of 65kDa. The cleaved forms of Angptl4, the C-terminal domain (47kDa) and the N-terminal domain (26kDa) were also detected. In human parenchymal fibroblasts the C-terminal domain was elevated by PDGF-BB in a time-dependent manner. The strongest expression was detected after 6 h of PDGF-BB stimulation. After 24 h PDGF-BB stimulation the C-Angptl4 expression was decreased again. The full-length form of Angptl4 and the N-terminal domain showed no change in protein level.

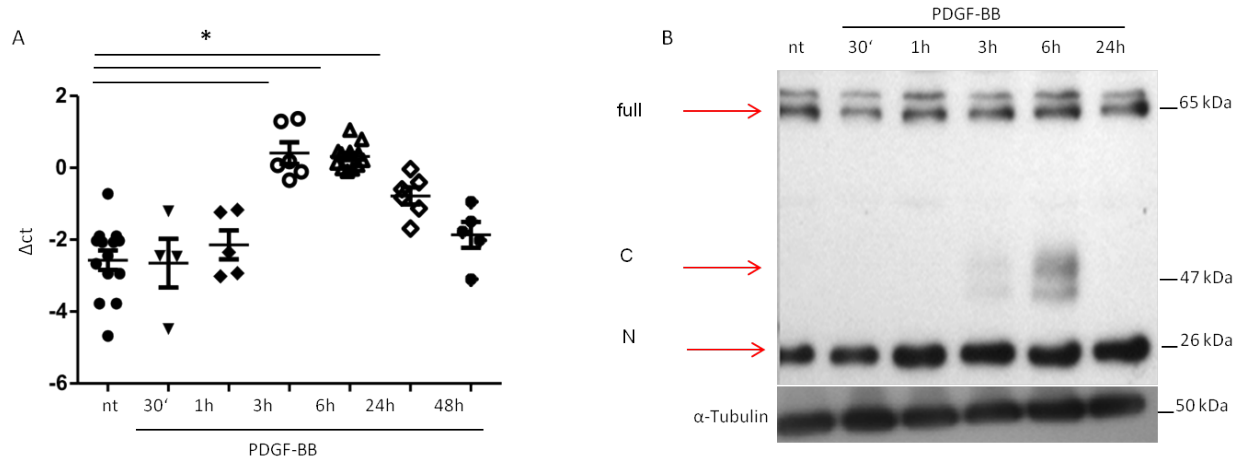


Figure 4.1: Expression of Angptl4 is elevated upon PDGF-BB stimulation in human parenchymal fibroblasts. (A) Real-time PCR analysis showed a time-dependent increase in Angptl4 expression. Human parenchymal fibroblasts were stimulated with 10 ng/ml PDGF-BB. One-way ANOVA, Tukey's Multiple Comparison Test; * $p < 0.05$; results are shown as mean with SEM; $n = 6$ each. (B) Western blot analyses of ANGPTL4 expression after 10 ng/ml PDGF-BB stimulation. C-terminal domain of Angptl4 is time-dependent regulated by PDGF-BB. Four independent western blots were performed. α -Tubulin shows the loading control. Angptl4: Angiopoietin-like 4; PDGF-BB: platelet-derived growth factor-BB; full: full-length Angptl4; C: C-terminal domain of Angptl4; N: N-terminal domain of Angptl4 nt: non treated; kDa: kilo dalton; ΔCt : delta cycle threshold; min: minute; h: hour.

In the next step we aimed to investigate whether the Angptl4 is secreted from human parenchymal fibroblasts. Therefore, we performed western blot analysis with the supernatant collected from cultured cells. Interestingly, in the supernatant of human parenchymal fibroblasts stimulated for 1 h with PDGF-BB we observed only higher levels of C-terminal domain Angptl4 as compared to the non-stimulated cells (figure 4.2). Staining of the gel with Croomassie brilliant Blue served as a loading control.

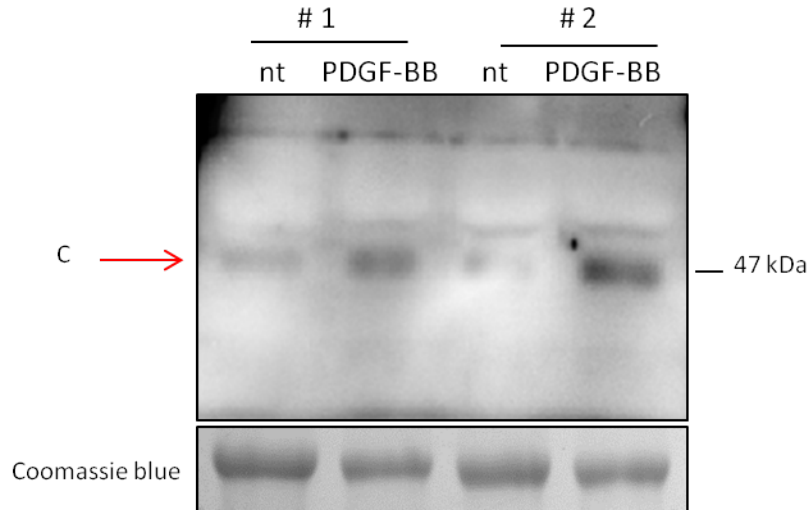


Figure 4.2: Human parenchymal fibroblasts secrete cleaved Angptl4. Supernatant of cells stimulated for 6 h with 10 ng/ml PDGF-BB were collected. Western blot analysis showed higher levels of C-terminal domain Angptl4 in the supernatant of human parenchymal fibroblasts. Two independent samples were used (# 1, # 2) Coomassie blue shows the loading control. PDGF-BB: platelet-derived growth factor-BB; C= C-terminal domain of Angptl4, nt= non-treated; kDa: kilo Dalton; h: hour.

4.2 MEK1/2 regulates the expression of Angptl4 in human parenchymal fibroblasts

To analyse which kinases are involved in the regulation of Angptl4 expression different pathways activated by PDGF-BB (MEK1/2, PI3K/Akt, JNK, p38) were inhibited. On the western blot the cleaved forms (C- and N- domain) of Angptl4 were detected (figure 4.3). The full-length form Angptl4 was not observed. The inhibition of MEK1/2 (U0126) decreased only the levels of the C-terminal domain Angptl4. The other inhibitors Wortmannin (PI3K/Akt kinase inhibitor), SP600126 (JNK inhibitor) and SB203580 (p38 inhibitor) had no effect of Angptl4 regulation.

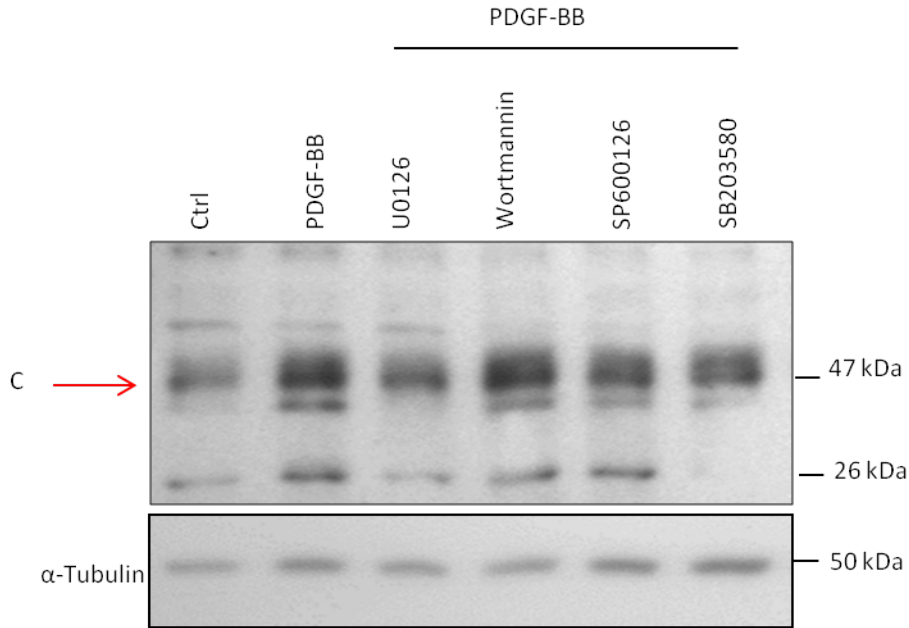


Figure 4.3: MEK1/2 regulates the expression of Angptl4 in human parenchymal fibroblasts. Western blot analysis of Angptl4 expression after inhibition with different inhibitors followed by 6 h stimulation with PDGF-BB (10ng/ml). Inhibitors: 50 μ M MEK1/2 (U0126), 80 μ M Wortmannin (PI3K/Akt kinase inhibitor), 5 μ M SP600126 (JNK inhibitor), 8 μ M SB203580 (p38 inhibitor). Ctrl (control): non-treated cells One of the three independent western blots is presented. α -Tubulin was used as a loading control. PDGF-BB: platelet-derived growth factor-BB; kDa: kilo dalton.

4.3 Cloning of the transcription factors Fra-2, JunB and cJun

To investigate if the transcriptions factors Fra-2, JunB and cJun play a role in the regulation of Angptl4, the transcriptions factors were cloned in a vector to overexpress them in human parenchymal fibroblasts.

4.3.1 Cloning of cJun in the expression vector (pcDNA3.1 (+))

First step was to produce a cJun fragment. The gradient PCR (figure 4.4) showed that the optimal annealing temperature to produce a cJun fragment (1000bp) was 56.5°C.

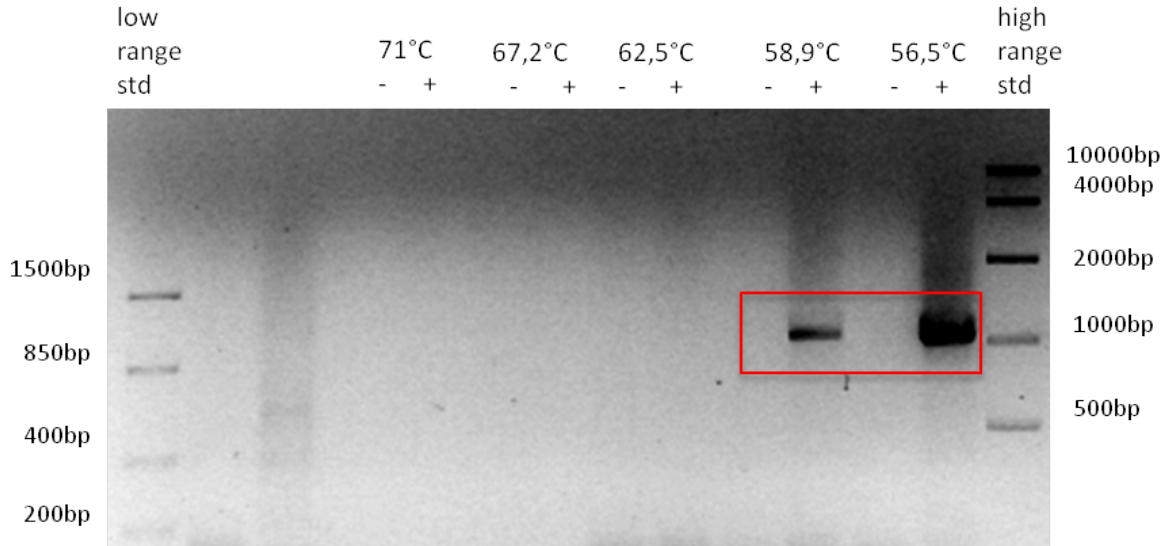


Figure 4.4: The cJun fragment has a size of 1000bp. The gradient PCR shows the optimal annealing temperature at 56.5°. The other annealing temperatures (71°C, 67.2°C, 62.5°C) did not show a PCR product. For each annealing temperature one negative control without cDNA (-) and the sample including the cDNA (+) was plotted. std: FastRuler™ standard; bp: base pairs.

For further PCRs the annealing temperature 56.5°C was used. All the samples except for sample 5 included the cJun fragment (figure 4.5). The negative control showed no band on the agarose gel as expected.

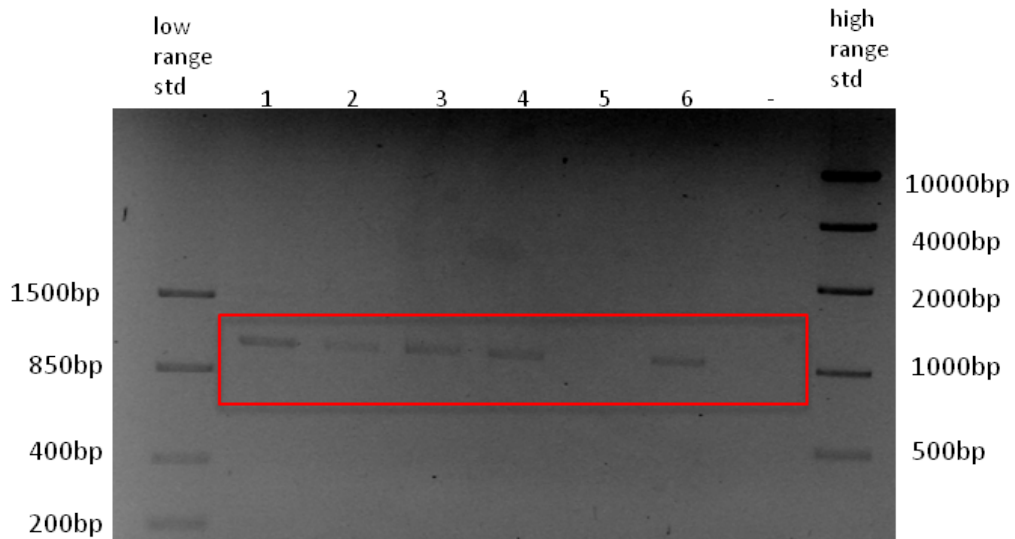


Figure 4.5: Establishment of the cJun fragment from a human cDNA. The samples (1-6) and one negative control without cDNA (-) was run by PCR. As a standard a low range standard and a high range standard were used. std: FastRuler™ standard; bp: base pairs.

The purified cJun fragment obtained in the optimized PCR and the plasmid pcDNA3.1(+) were cut with the restriction enzymes EcoRI and XhoI (figure 4.6). Subsequently the cJun fragment was ligated with the plasmid pcDNA3.1(+).

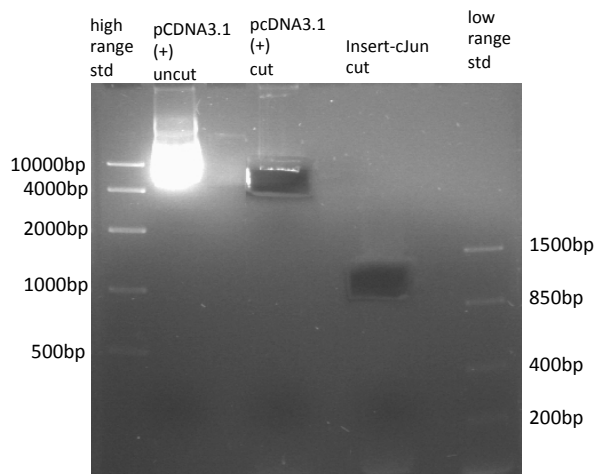


Figure 4.6: Gel electrophoresis showed the pcDNA3.1(+) and cJun fragment cut by EcoRI and XhoI. As a control the uncut vector pcDNA3.1(+) was loaded. std: FastRuler™ standard; bp: base pairs.

4.3.2 Transformation of vector complexes in *E.coli*

The transformation of the vector complexes CMV-hu-Fra-2 [pcDNA3] and pGEMT-hu-JunB in NEB5- α competent *E.coli* was successful. The vector complex CMV-hu-cJun [pcDNA3.1] in NEB5- α competent *E.coli* showed no colonies. Since the positiv control showed also no colonies, we supposed there were problems with the used pcDNA3.1 vector. The following experiments were done without CMV-hu-cJun [pcDNA3.1]. Cloning of cJun will be repeated with different expression vector construct to creat a working hu-cJun expression vector.

As a control whether the transformation vector includes the correct insert (JunB and Fra-2) a restriction analysi of the insert and a sequencing of the transformed vector complexes CMV-hu-Fra-2 [pcDNA3] and pGEMT-hu-JunB was done.

Since we did not know the exact DNA-sequence and therefore the accurate restriction sites in the vector, but we knew the restriction sites in the insert gen, the restriction enzyme AvaII (CMV-hu-Fra-2 [pcDNA3]) and BsaHI (pGEMT-hu-JunB) were used. The restriction of CMV-hu-Fra-2 [pcDNA3] showed four fragments with a size of 200bp, 750bp, 1900bp and 2200bp (figure 4.7). The

200bp band was the cutting product of Fra-2 gen. The restriction of pGEMT-hu-JunB with the enzyme BsaHI constituted two fragments with a size of 1900bp and 1100bp.

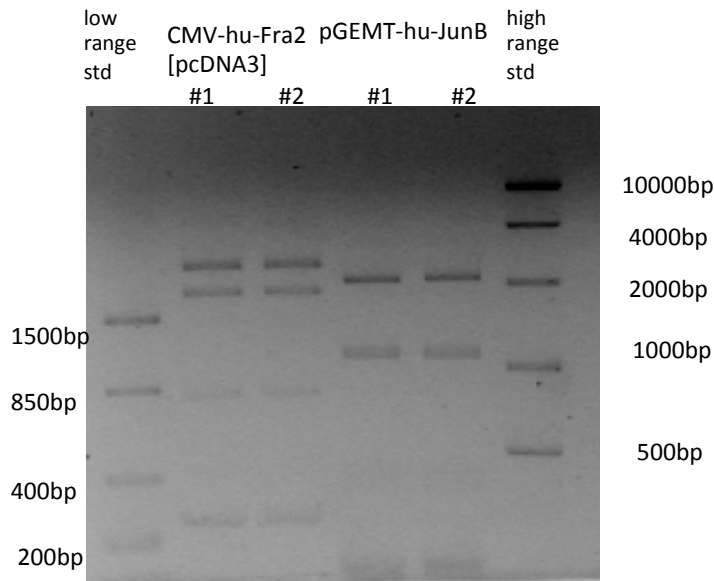


Figure 4.7: The Restriction result of CMV-hu-Fra-2 [pcDNA3] cut by A_{va}II and pGEMT-hu-JunB cut by BsaHI The restriction of the vector complexes shows that the inserts were successfully cloned in the plamids. The gel electrophoresis of the CMV-hu-Fra-2 [pcDNA3] restriction (A_{va}II) showed 4 bands (200bp,750bp,1900bp,2200bp) and the gel electrophoresis of the pGEMT-hu-JunB restriction (BsaHI) showed 2 bands (1900bp, 1100bp). For each vector two restriction preparations (#1 and #2) were done. As a standard a low range standard and a high range standard were used. std: FastRuler™ standard; bp: base pairs.

The sequencing comfimed that the vectors include the correct Fra-2 and JunB genes without mutations.

4.4 AP-1 complex has no significant effect on Angptl4 expression in human parenchymal fibroblasts

We hypothesized that JunB, cJun, cFos and Fra-2 are transcription factors involved in Angptl4 expression in human parenchymal fibroblasts. In order to understand if these AP-1 components are involved in Angptl4 regulation, they were silenced and the Angptl4 expression was measured. The experiments were performed without and with 1 h PDGF-BB stimulation. The Real-time PCR results showed no significant impact of AP-1 silencing on Angptl4 expression (figure 4.8A). The results of silencing experiments for JunB, cJun, Fra-2 and cFos were heterogeneous. No effect on Angptl4

expression was also observed after silencing of AP-1 components upon PDGF-BB stimulation (figure 4.8B).

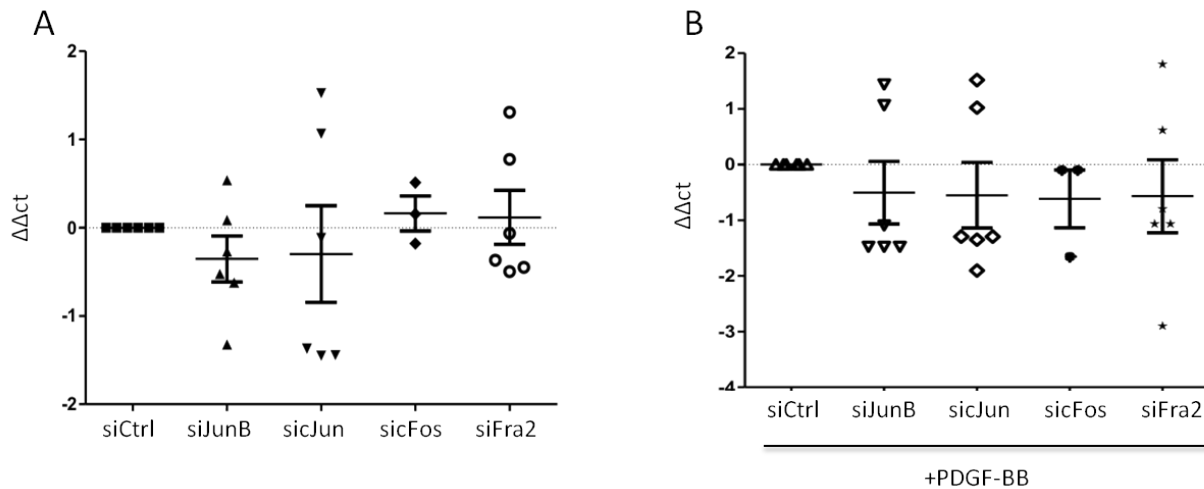


Figure 4.8: Silencing of AP-1 complex has no significant effect on Angptl4 expression in human parenchymal fibroblasts. (A) Real-time PCR analysis of Angptl4 expression after silencing of the transcription factors JunB, cJun, cFos, Fra-2 (B) mRNA levels of Angptl4 after silencing of the transcript factors JunB, cJun, Fra-2 and cFos followed by 1 h stimulation with 10 ng/ml PDGF-BB. Results are normalized to the reference genes B2M and PBGD. One-way ANOVA, Tukey's Multiple Comparison Test. PDGF-BB: platelet-derived growth factor-BB; siCtrl: silencing control; $\Delta\Delta Ct$: delta delta cycle threshold; h: hour.

4.5 Angptl4 has an effect on proliferation of human parenchymal fibroblasts

The silencing efficiency of Angptl4 was performed on mRNA and protein levels. The knock-down of Angptl4 leads to decreased Angptl4 expression on the mRNA level. Western blot analysis showed that siAngptl4 had only an effect on C-terminal domain of Angptl4. We observed that silencing of Angptl4 (siAngptl4) led to a significant decrease of proliferation in human parenchymal fibroblasts (figure 4.8). This lower proliferation was monitored in non-stimulated cells as well as in the PDGF-BB cells.

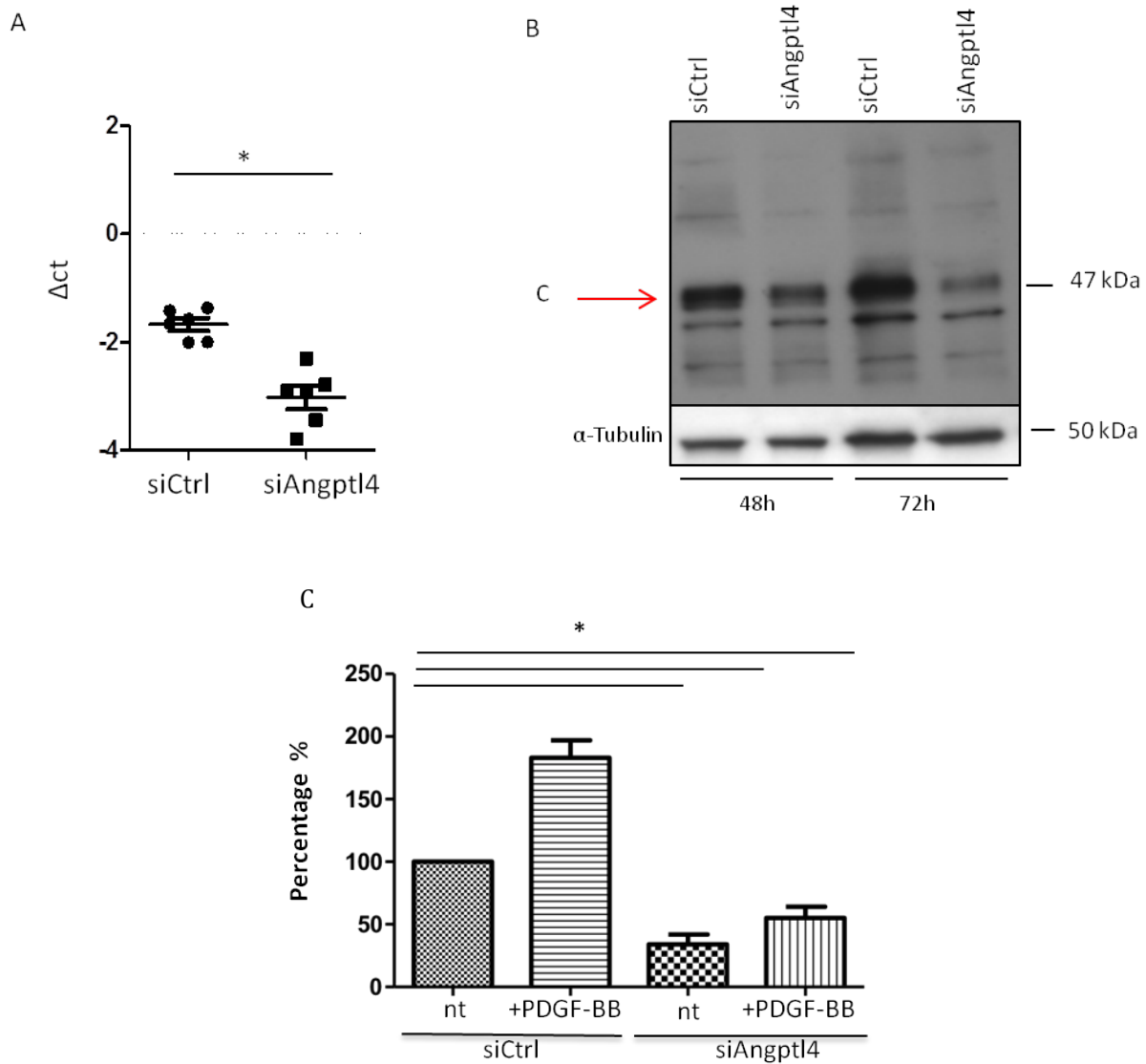


Figure 4.9: siAngptl4 decreased the proliferation of human parenchymal fibroblasts. Silencing control of Angptl4 on mRNA level (A) and on protein level (B). Unpaired t-test; *P<0.05; results are shown as mean with SEM (C) Proliferation assay of silenced Angptl4 cells stimulated with 10 ng/ml PDGF-BB (+PDGF-BB) for 24 h. siCtrl served as a silencing control. nt= non-PDGF-BB stimulated. Proliferation assay was performed with human parenchymal fibroblast from 5 different healthy donors primary cells. One-way ANOVA, Tukey's Multiple Comparison Test; *P<0.05; results are shown as mean with SEM. PDGF-BB: platelet-derived growth factor-BB; Angptl4: Angiopoietin- like 4 siCtrl: silencing control; nt: non- treated; h: hour.

5 Discussion

In this study we investigated the upstream signaling of Angptl4 and its role in the regulation of human parenchymal fibroblast proliferation.

We observed that Angptl4 is expressed in human parenchymal fibroblasts. As a major Angptl4 upstream signaling regulator we detected the pro-proliferative factor PDGF-BB. PDGF-BB leads to a time-dependent increase of Angptl4 expression with a peak after 6 h. Binding of PDGF-BB to its receptor activates the kinase MEK1/2 in human fibroblast and leads to the expression of Angptl4. In our study we could not acknowledge that the transcription factor AP-1 complex is involved in the regulation of Angptl4 expression (figure 5.1).

It is known that full-length Angptl4 can be proteolytically cleaved by proprotein convertases such as furin into an N-terminal coiled-coil domain and C-terminal fibrinogen-like domain [56]. Several studies could confirm that the cleavage of Angptl4 is tissue dependent [56]. The two domains have different function after the proteolytic cleavage. The C-terminal domain interacts with ECM proteins and integrins and the N-terminal domain is associated with lipid metabolism [51-55]. In human parenchymal fibroblasts we detected all three forms of Angptl4. However, we saw only a time-dependent increase of the C-terminal domain level after PDGF-BB stimulation. The full-length Angptl4 and the N-terminal domain were largely unaffected. So far we do not know why only the C-terminal domain is regulated by PDGF-BB. One possibility is that the used anti-hANGPTL4 antibody can only recognize the C-terminal and not the other two forms. We monitored the antibody by silencing Angptl4 and saw that predominantly the bands of the C-terminal domain disappeared. This result indicates that the anti-hANGPTL4 antibody could only be specific for the C-terminal domain. To confirm our speculation the experiments with other antibodies should be performed. A further factor, which has to be tested, is the stability of the two domains. So far there is only little known about the stability of Angptl4. Yin W. et al. wrote in his publication about the stability of N-terminal domain. He investigated that the N-terminal domain is only stable if it interacts with LPL [53]. Perhaps in human parenchymal fibroblasts the N-terminal domain is not as stable as the C-terminal domain. This can also constitute why the N-terminal domain is not affected after PDGF-BB stimulation.

Since the growth factor PDGF-BB activates several kinases, which are involved in regulation of cell growth and survival [29, 30] we explored four kinase pathways. The kinases PI3K/Akt, JNK and p38 had no effect of the Angptl4 expression. It seems that Angptl4 expression was regulated through the Ras/MEK/ERK1/2 MAPK pathway. This level change was again only seen at the C-terminal domain and not in the other two forms of Angptl4. The reasons are the same as above described. Yang et al. discovered that C-Angptl4 inhibits the MEK1/2 MAPK pathway by inactivation of Raf-1 [26]. This inactivation leads to angiogenesis inhibition in human endothelial cells. They also observed that Angptl4 has no effect on Akt and p38 MAP kinase in human endothelial cells [26]. So far we did not investigate if Angptl4 affects some of the kinases (Akt, JNK, p38, MEK1/2) in human parenchymal fibroblasts. Nevertheless it is most likely that this is the case and Angptl4 regulates MEK1/2 in a similar manner as in human endothelial cells. It seems that Angptl4 regulates its own PDGF-BB induced expression by inhibition of MEK1/2. However, this is only speculation and has to be proven. Another study by Noh JM et al. shows that the inhibition of JNK reduced IL-1 β induced Angptl4 expression in osteoblastic cells. On the other hand the inhibition of p38 and ERK1/2 shows no effect [63].

Several studies could show that PDGF-BB induced Ras/MEK/ERK1/2 MAPK regulates the transcription factor AP-1 [29-31]. The AP-1 complex is involved in the regulation of cell proliferation [64]. Pal M. et al. demonstrated that Angptl4 influences the activation of AP-1 complex in epidermal differentiation. Angptl4 leads to an increase of c-Jun and JunB expression [61]. In our study we determined that AP-1 complex has no effect on Angptl4 expression in human parenchymal fibroblasts. This experiment should be repeated as our results diversify a lot, and were therefore not significant. In an ongoing experiment we started to prove if an overexpression of AP-1 complex effects Angptl4 expression in fibroblasts. MEK1/2 kinase activates AP-1 complex, which could be a transcription factor for Angptl4 in human parenchymal fibroblast.

In addition, we observed that only the C-terminal domain is secreted by human fibroblasts. This means the cleavage has do happen inside the cells. We determined that if we stimulated the cells with PDGF-BB the level of the secreted C-terminal domain was increased. After the secretion, the C-terminal domain can interact with integrins and ECM proteins. It is known that in keratinocytes the C-terminal domain is secreted and subsequently interacts with integrins and ECM proteins such as vitronectin and fibronectin [54,55]. The specific binding to the integrins activates the transcription factor AP-1, which regulates the epidermal differentiation and proliferation [61]. The described signaling mechanism could be also a possible in human parenchymal fibroblast. However, the exact role of the secreted C-terminal domain is not completely understood.

Goh et al identified Angptl4 as an ECM component, which plays a role in cell-matrix communication, and influences wound healing [55]. This study is a first indication that Angptl4 could be a profibrotic factor which may play a role in the pathogenesis of IPF [8]. IPF is characterized by massive proliferation of parenchymal fibroblasts and an irreversible accumulation of connective tissue in the interstitium of the lung. The lung becomes thick, stiff and scarred over time [8, 33]. The pathobiology is not well understood. It is known that ECM molecules have been implicated in the pathobiology of IPF [8]. In our study we investigated that Angptl4 stimulates the proliferation of fibroblasts, which with a high probability may lead to an excessive proliferation and to the development of lung diseases such as IPF. So far we could not identify the exact role of Angptl4 in IPF and many questions are still unanswered. For example we do not know which role the three forms of Angptl4 play in IPF. In this current study it seems that only the C-terminal domain is regulated in human parenchymal fibroblasts and not the other two Angptl4 forms. Nevertheless, so far we can not exclude that the full-length Angptl4 and N-terminal domain play also a role in the pathogenesis of IPF. It is possible that both domains have contrary functions in the pathogenesis of IPF. The C-terminal domain might lead to a pro-fibrotic phenotype and the N-terminal domain may protect against fibrosis. However, as long as we do not know if both domains of Angptl4 are involved in IPF, we can only speculate about the function of Angptl4 in human parenchymal fibroblasts.

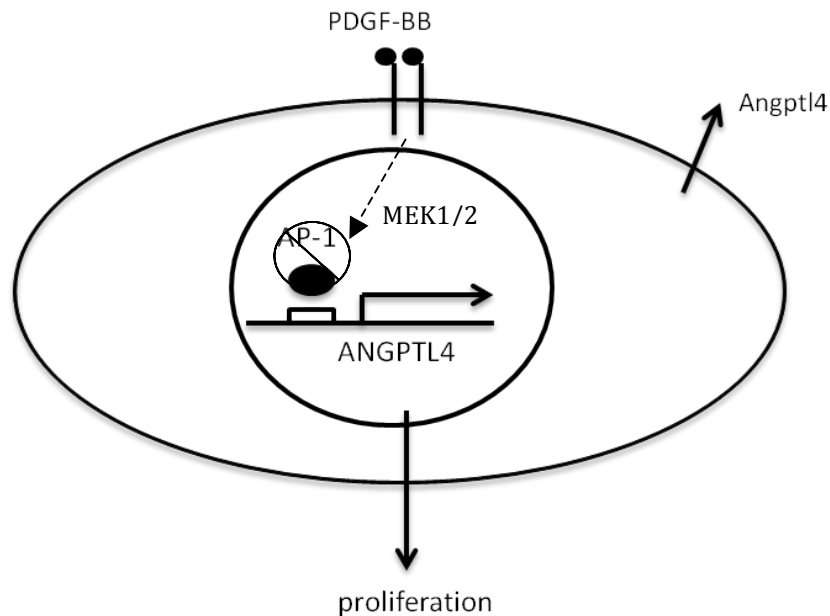


Figure 5.1: Schematic representation of the upstream signaling from Angptl4 in human fibroblasts. Angptl4 leads to proliferation of fibroblasts and can be secreted.

5.1 Outlook

In this study we investigate the PDGF-BB induced upstream signaling of Angptl4 which leads to proliferation in human parenchymal fibroblasts. In order to prove the possible role of Angptl4 as a profibrotic factor in the pathogenesis of IPF further experiments have to be done. First of all we have to localize Angptl4 in the lung tissue. Therefore we need a good antibody. Furthermore, it has to be investigated, which phenotype Angptl4 overexpression or Angptl4 knockout mice show in bleomycin-induced lung fibrosis mouse model. The functions of the two Angptl4 domains have to be clarified. This can be done by using an N-terminal domain and a C-terminal domain specific antibody or create mice, which express only one Angptl4 domain. In addition, the influence of other profibrotic factors such as the transforming growth factor- β (TGF- β) on Angptl4 expression has to be explored. Figure 5.2 shows the potential role of Angptl4 in the development of IPF.

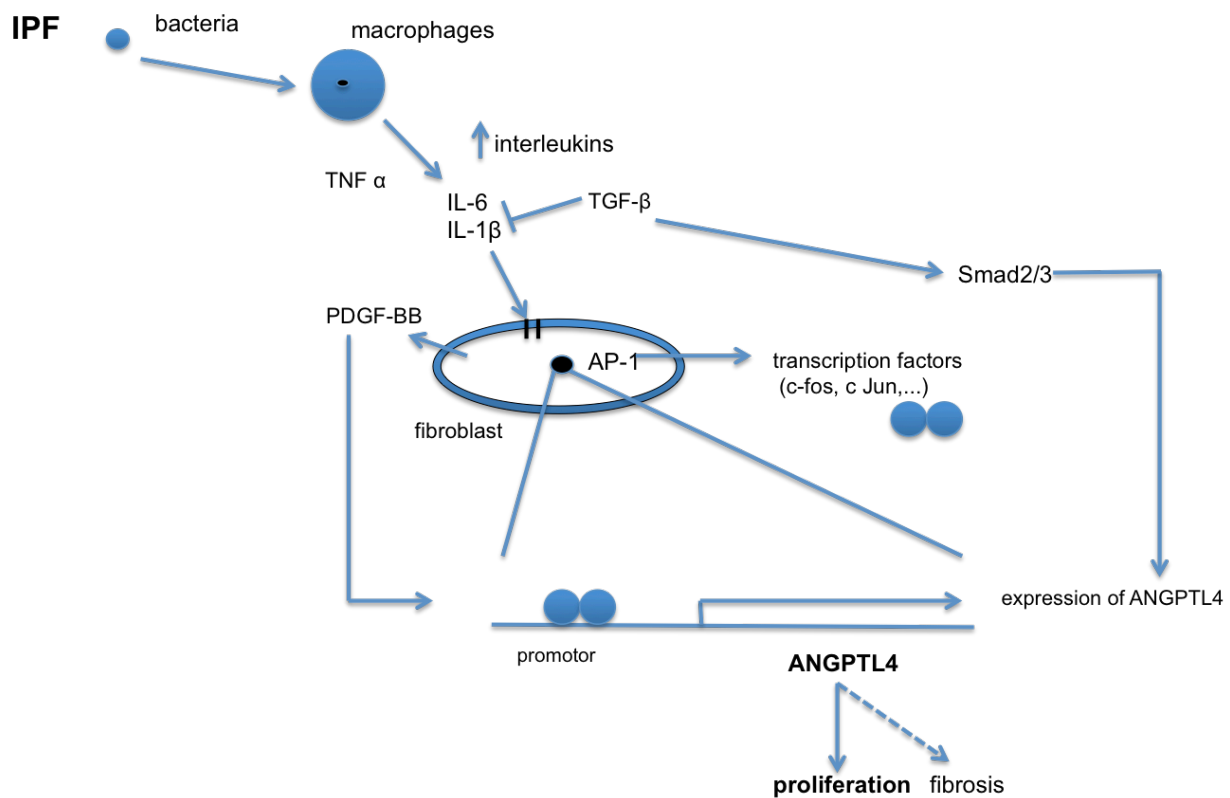


Figure 5.2: Schematic figure summarizing possible Angptl4 involvement in the pathogenesis of IPF.

6 Supplement

Created with SnapGene®

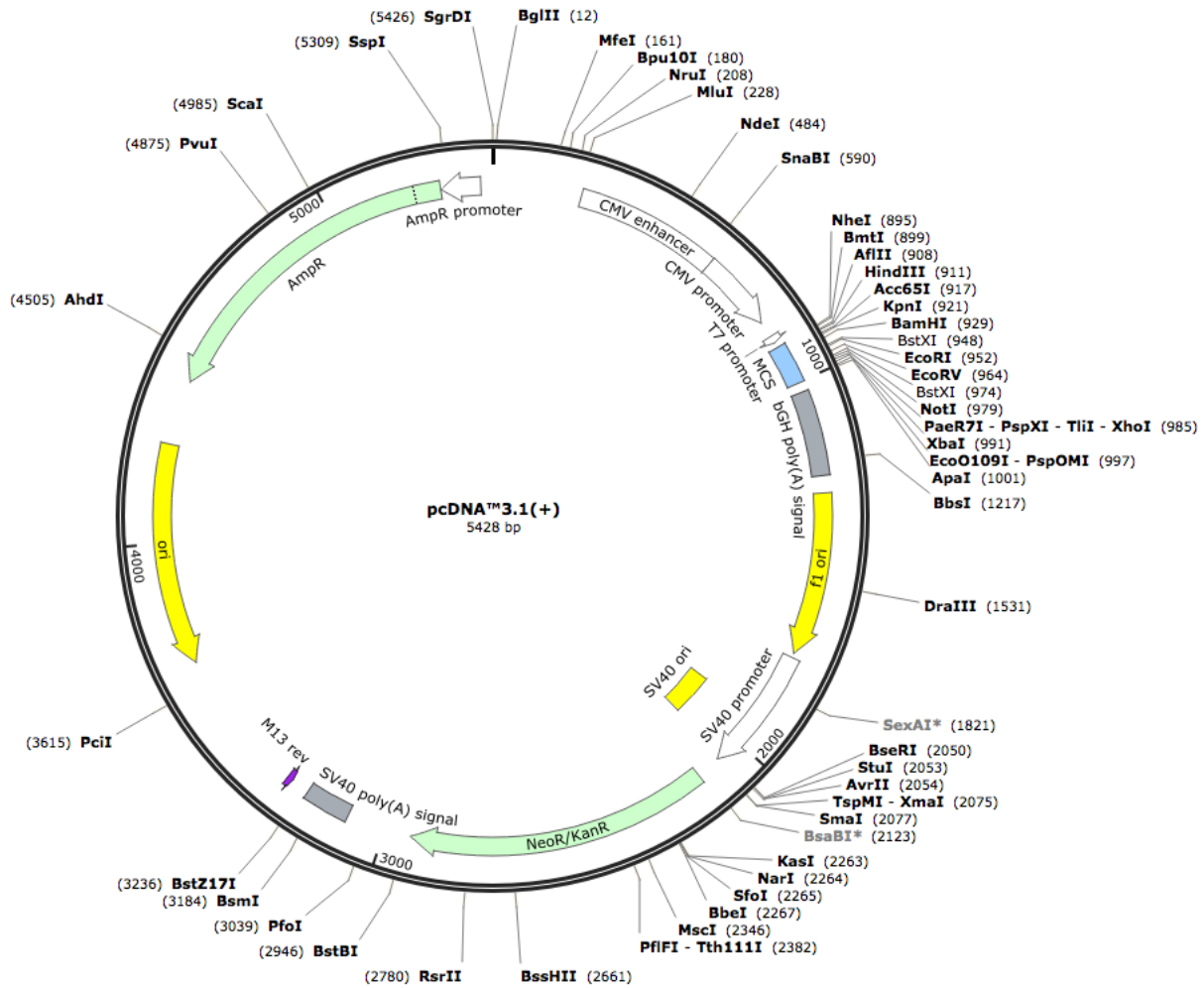


Figure 6.1: pcDNA 3.1(+) vector map.

([https://www.snapgene.com/resources/plasmid_files/basic_cloning_vectors/pcDNA3.1\(+\)/](https://www.snapgene.com/resources/plasmid_files/basic_cloning_vectors/pcDNA3.1(+)/))

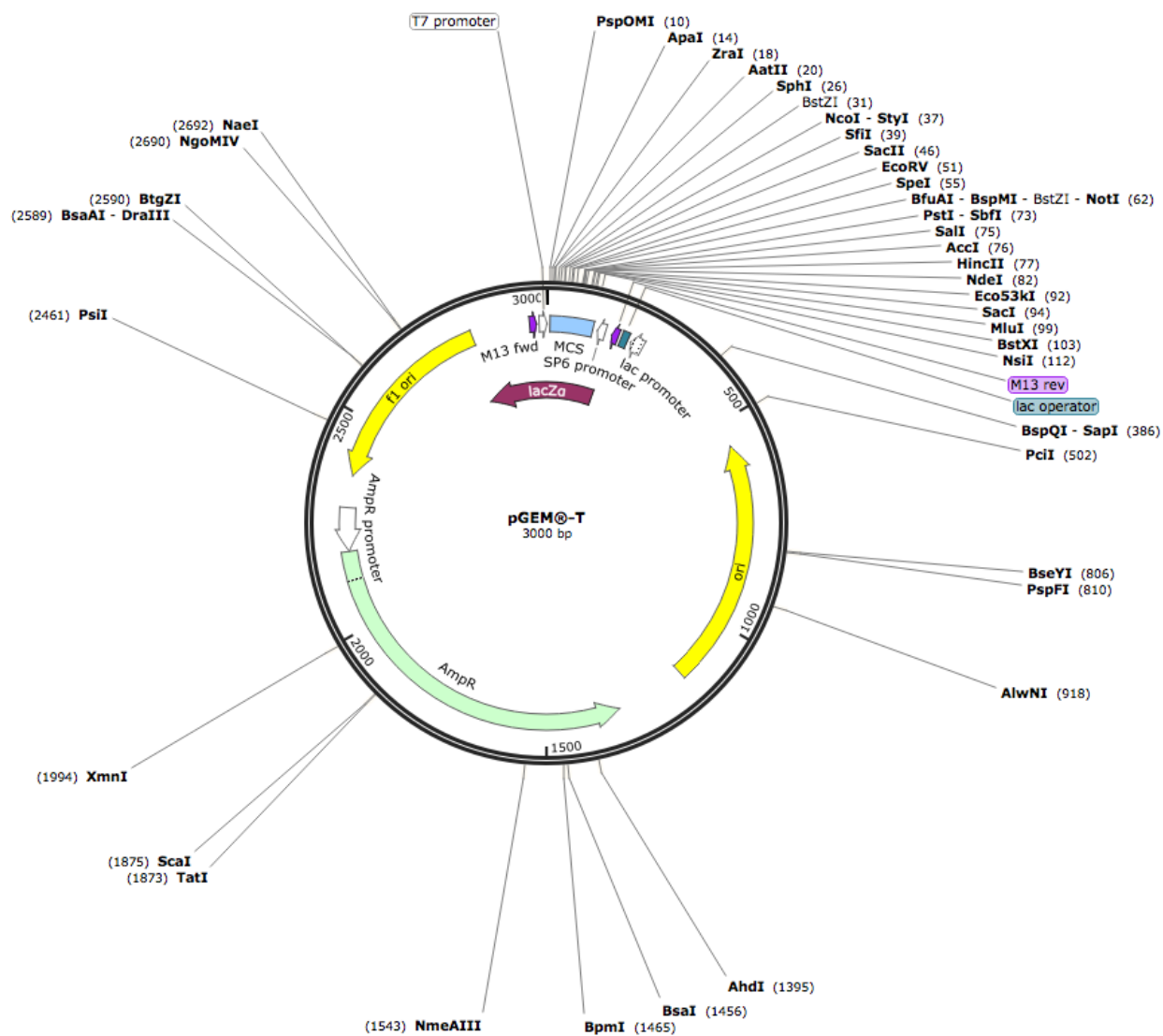


Figure 6.2: pGEM-T vector map.

https://www.snapgene.com/resources/plasmid_files/basic_cloning_vectors/pGEM-T/

JunB:

>gi|44921611|ref|NM_002229.2| Homo sapiens jun B proto-oncogene (JUNB), mRNA
CDS 277..1320 (1044 bp)

```
GAGCGGCCAGGCCAGCCTCGGAGCCAGCAGGGAGCTGGGAGCTGGGGGAAACGACGCCAGGAAAGCTATCGCGCCAGA
GAGGGCGACGGGGGCTCGGGAAGCCTGACAGGGCTTTTGCACAGCTGCCGGCTGGCTGCTACCCGCCCGCCAGC
CCCCGAGAACCGCGCACCAGGCACCCAGTCCGGTCAACGACGGAGAGCTCGCCGCTCGCTGCAGCGAGGCCCGGAG
CGGCCCCGCAGGGACCCCTCCCCAGACCGCTGGGCCGCCCGGATGACTGACTAAAATGGAACAGCCCTTCTACCACGAC
GACTCATAACAGCTACGGGATACGGCCGGGCCCCCTGGTGGCCTCTCTTACACGACTACAACTCCTGAAACCGAGC
CTGGCGGTCAACCTGGCCGACCCCTACCGGAGTCTCAAAGCGCTGGGGCTCGCGGACCCGGCCAGAGGGCGGGCGGT
GGCGGCAGCTACTTTTCTGGTCAAGGCTCGGACACCGGCGCTCTCTCAAGCTCGCCTCTTCGGAGCTGGAACGCCCTG
ATTGTCCCCAACAGCAACGGCGTGATCAGCAGCGCCCTACACCCCGGGACAGTACTTTTACCCCGCGGGGGTGGC
AGCGGTGGAGGTGCAGGGGGCGCAGGGGGCGGGCTCACCGAGGAGCAGGAGGGCTTCGCCGACGGCTTTGTCAAAGCC
CTGGACGATCTGCACAAGATGAACCACGTGACACCCCAACGTGTCCCTGGGCGCTACCGGGGGGGCCCCCGGCTGGG
CCCGGGGGCGTCTACGCCGGCCCGGAGCCACCTCCCGTTTACACCAACCTCAGCAGCTACTCCCCAGCCTCTGCGTCC
TCGGGAGGCGCCGGGGCTGCCGTGGGACCGGGAGCTCGTACCCGACGACCACCATCAGCTACTCCACACGCGCCG
CCCTTCGCCGTGGCCACCCGGCGCAGCTGGGTGGGGCCGGCGCCCTCCACCTTCAAGGAGGAACCGCAGACCGTG
CCGAAGCGCGCAGCCGGGACGCCACGCGCCGTTGCCCATCAACATGGAAGACCAAGAGCGCATCAAAGTGGAG
CGAAGCGGCTGCAGGAACCGCTGGCGGCCACCAAGTGCCGGAAGCGGAAGCTGGAGCGCATCGCGCGCCTGGAGGAC
AAGGTGAAGACGCTCAAGGCCGAGAACGCGGGGCTGTGAGTACCGCCGGCTCCTCCGGGAGCAGGTGGCCAGCTC
AAACAGAAGGTCATGACCCACGTGAGCAACGGCTGTGAGCTGCTGCTTGGGGTCAAGGGACACGCCCTTCTGAACGTCC
CTGCCCCCTTTACGGACACCCCTCGCTTGGACGGCTGGGCACACGCCCTCCACTGGGGTCCAGGGAGCAGGCGGTGG
GCACCCACCCCTGGGACCTAGGGGCGCCGAAACCACACTGGACTCCGGCCCTCCTACCCCTGCGCCCAGTCCTTCCACC
TCGACGTTTACAAGCCCCCTTCCACTTTTTTTTTGTATGTTTTTTTTCTGCTGGAAACAGACTCGATTATATTTGAA
TATAATATATTTGTGTATTTAACAGGGAGGGGAAGAGGGGGCGATCGCGGCGGAGCTGGCCCCGCCGCTGGTACTCA
AGCCCGGGGACATTTGGGAAGGGGACCCCGCCCCCTGCCCTCCCTCTCTGCACCGTACTGTGAAAAGAAACACG
CACTTAGTCTCTAAAGAGTTTATTTTAAGACGTGTTTGTGTTTGTGTGTTTGTTCCTTTTTTATTGAATCTATTTAAG
TAAAAAAAAAATTTGGTTCTTTAAAAAAAAAAAAAAAAAAAA
```

JunB_fw:

GGACGATCTGCACAAGATG

JunB_rv: (reverse complement)

GTTCCCTCCTTGAAGGTGGA

JunB_rv_2: (reverse complement)

TGTAGGCGTCGTCGTGAT

7 Reference

1. King TE, Jr., Pardo A, Selman M. Idiopathic pulmonary fibrosis. *Lancet* 2011; 378(9807): 1949-1961.
2. Kanekar S, Hirozanne T, Terracio L, Borg TK. Cardiac fibroblasts form and function. *Cardiovascular pathology : the official journal of the Society for Cardiovascular Pathology* 1998; 7(3): 127-133.
3. Kendall RT, Feghali-Bostwick CA. Fibroblasts in fibrosis: novel roles and mediators. *Frontiers in pharmacology* 2014; 5: 123.
4. Singer AJ, Clark RA. Cutaneous wound healing. *The New England journal of medicine* 1999; 341(10): 738-746.
5. Feghali CA, Wright TM. Cytokines in acute and chronic inflammation. *Frontiers in bioscience : a journal and virtual library* 1997; 2: d12-26.
6. Porter KE, Turner NA. Cardiac fibroblasts: at the heart of myocardial remodeling. *Pharmacology & therapeutics* 2009; 123(2): 255-278.
7. Scotton CJ, Chambers RC. Molecular targets in pulmonary fibrosis: the myofibroblast in focus. *Chest* 2007; 132(4): 1311-1321.
8. Katzenstein AL, Myers JL. Idiopathic pulmonary fibrosis: clinical relevance of pathologic classification. *American journal of respiratory and critical care medicine* 1998; 157(4 Pt 1): 1301-1315.
9. Ross R, Raines EW, Bowen-Pope DF. The biology of platelet-derived growth factor. *Cell* 1986; 46(2): 155-169.
10. Pierce GF, Tarpley JE, Tseng J, Bready J, Chang D, Kenney WC, Rudolph R, Robson MC, Vande Berg J, Reid P, et al. Detection of platelet-derived growth factor (PDGF)-AA in actively healing human wounds treated with recombinant PDGF-BB and absence of PDGF in chronic nonhealing wounds. *The Journal of clinical investigation* 1995; 96(3): 1336-1350.
11. Heldin CH, Westermark B. Mechanism of action and in vivo role of platelet-derived growth factor. *Physiological reviews* 1999; 79(4): 1283-1316.
12. Kohler N, Lipton A. Platelets as a source of fibroblast growth-promoting activity. *Experimental cell research* 1974; 87(2): 297-301.
13. Ross R, Glomset J, Kariya B, Harker L. A platelet-dependent serum factor that stimulates the proliferation of arterial smooth muscle cells in vitro. *Proceedings of the National Academy of Sciences of the United States of America* 1974; 71(4): 1207-1210.
14. Nister M, Heldin CH, Wasteson A, Westermark B. A glioma-derived analog to platelet-derived growth factor: demonstration of receptor competing activity and immunological crossreactivity. *Proceedings of the National Academy of Sciences of the United States of America* 1984; 81(3): 926-930.

15. Fredriksson L, Li H, Eriksson U. The PDGF family: four gene products form five dimeric isoforms. *Cytokine & growth factor reviews* 2004; 15(4): 197-204.
16. Abramsson A, Kurup S, Busse M, Yamada S, Lindblom P, Schallmeiner E, Stenzel D, Sauvaget D, Ledin J, Ringvall M, Landegren U, Kjellen L, Bondjers G, Li JP, Lindahl U, Spillmann D, Betsholtz C, Gerhardt H. Defective N-sulfation of heparan sulfate proteoglycans limits PDGF-BB binding and pericyte recruitment in vascular development. *Genes & development* 2007; 21(3): 316-331.
17. Lindblom P, Gerhardt H, Liebner S, Abramsson A, Enge M, Hellstrom M, Backstrom G, Fredriksson S, Landegren U, Nystrom HC, Bergstrom G, Dejana E, Ostman A, Lindahl P, Betsholtz C. Endothelial PDGF-B retention is required for proper investment of pericytes in the microvessel wall. *Genes & development* 2003; 17(15): 1835-1840.
18. McDonald NQ, Hendrickson WA. A structural superfamily of growth factors containing a cystine knot motif. *Cell* 1993; 73(3): 421-424.
19. Seidah NG, Prat A. The biology and therapeutic targeting of the proprotein convertases. *Nature reviews Drug discovery* 2012; 11(5): 367-383.
20. Chen PH, Chen X, He X. Platelet-derived growth factors and their receptors: structural and functional perspectives. *Biochimica et biophysica acta* 2013; 1834(10): 2176-2186.
21. Hart CE, Forstrom JW, Kelly JD, Seifert RA, Smith RA, Ross R, Murray MJ, Bowen-Pope DF. Two classes of PDGF receptor recognize different isoforms of PDGF. *Science* 1988; 240(4858): 1529-1531.
22. Heldin CH, Backstrom G, Ostman A, Hammacher A, Ronnstrand L, Rubin K, Nister M, Westermark B. Binding of different dimeric forms of PDGF to human fibroblasts: evidence for two separate receptor types. *The EMBO journal* 1988; 7(5): 1387-1393.
23. Matsui T, Pierce JH, Fleming TP, Greenberger JS, LaRochelle WJ, Ruggiero M, Aaronson SA. Independent expression of human alpha or beta platelet-derived growth factor receptor cDNAs in a naive hematopoietic cell leads to functional coupling with mitogenic and chemotactic signaling pathways. *Proceedings of the National Academy of Sciences of the United States of America* 1989; 86(21): 8314-8318.
24. Chiara F, Bishayee S, Heldin CH, Demoulin JB. Autoinhibition of the platelet-derived growth factor beta-receptor tyrosine kinase by its C-terminal tail. *The Journal of biological chemistry* 2004; 279(19): 19732-19738.
25. Demoulin JB, Montano-Almendras CP. Platelet-derived growth factors and their receptors in normal and malignant hematopoiesis. *American journal of blood research* 2012; 2(1): 44-56.
26. Yang YH, Wang Y, Lam KS, Yau MH, Cheng KK, Zhang J, Zhu W, Wu D, Xu A. Suppression of the Raf/MEK/ERK signaling cascade and inhibition of angiogenesis by the carboxyl terminus of angiopoietin-like protein 4. *Arteriosclerosis, thrombosis, and vascular biology* 2008; 28(5): 835-840.
27. Yuzawa S, Opatowsky Y, Zhang Z, Mandiyan V, Lax I, Schlessinger J. Structural basis for activation of the receptor tyrosine kinase KIT by stem cell factor. *Cell* 2007; 130(2): 323-334.

28. Kazlauskas A, Cooper JA. Autophosphorylation of the PDGF receptor in the kinase insert region regulates interactions with cell proteins. *Cell* 1989; 58(6): 1121-1133.
29. Essaghir A, Toffalini F, Knoops L, Kallin A, van Helden J, Demoulin JB. Transcription factor regulation can be accurately predicted from the presence of target gene signatures in microarray gene expression data. *Nucleic acids research* 2010; 38(11): e120.
30. Fambrough D, McClure K, Kazlauskas A, Lander ES. Diverse signaling pathways activated by growth factor receptors induce broadly overlapping, rather than independent, sets of genes. *Cell* 1999; 97(6): 727-741.
31. Choudhury GG, Karamitsos C, Hernandez J, Gentilini A, Bardgett J, Abboud HE. PI-3-kinase and MAPK regulate mesangial cell proliferation and migration in response to PDGF. *The American journal of physiology* 1997; 273(6 Pt 2): F931-938.
32. Scherping SC, Jr., Schmidt CC, Georgescu HI, Kwoh CK, Evans CH, Woo SL. Effect of growth factors on the proliferation of ligament fibroblasts from skeletally mature rabbits. *Connective tissue research* 1997; 36(1): 1-8.
33. Andrae J, Gallini R, Betsholtz C. Role of platelet-derived growth factors in physiology and medicine. *Genes & development* 2008; 22(10): 1276-1312.
34. Bonner JC. Regulation of PDGF and its receptors in fibrotic diseases. *Cytokine & growth factor reviews* 2004; 15(4): 255-273.
35. Bonner JC, Goodell AL, Coin PG, Brody AR. Chrysotile asbestos upregulates gene expression and production of alpha-receptors for platelet-derived growth factor (PDGF-AA) on rat lung fibroblasts. *The Journal of clinical investigation* 1993; 92(1): 425-430.
36. Clement LC, Avila-Casado C, Mace C, Soria E, Bakker WW, Kersten S, Chugh SS. Podocyte-secreted angiopoietin-like-4 mediates proteinuria in glucocorticoid-sensitive nephrotic syndrome. *Nature medicine* 2011; 17(1): 117-122.
37. Kim I, Kim HG, Kim H, Kim HH, Park SK, Uhm CS, Lee ZH, Koh GY. Hepatic expression, synthesis and secretion of a novel fibrinogen/angiopoietin-related protein that prevents endothelial-cell apoptosis. *The Biochemical journal* 2000; 346 Pt 3: 603-610.
38. Hato T, Tabata M, Oike Y. The role of angiopoietin-like proteins in angiogenesis and metabolism. *Trends in cardiovascular medicine* 2008; 18(1): 6-14.
39. Dutton S, Trayhurn P. Regulation of angiopoietin-like protein 4/fastig-inducible adipose factor (Angptl4/FIAF) expression in mouse white adipose tissue and 3T3-L1 adipocytes. *The British journal of nutrition* 2008; 100(1): 18-26.
40. Yu X, Burgess SC, Ge H, Wong KK, Nasseem RH, Garry DJ, Sherry AD, Malloy CR, Berger JP, Li C. Inhibition of cardiac lipoprotein utilization by transgenic overexpression of Angptl4 in the heart. *Proceedings of the National Academy of Sciences of the United States of America* 2005; 102(5): 1767-1772.

41. Staiger H, Haas C, Machann J, Werner R, Weisser M, Schick F, Machicao F, Stefan N, Fritsche A, Haring HU. Muscle-derived angiopoietin-like protein 4 is induced by fatty acids via peroxisome proliferator-activated receptor (PPAR)-delta and is of metabolic relevance in humans. *Diabetes* 2009; 58(3): 579-589.
42. Backhed F, Ding H, Wang T, Hooper LV, Koh GY, Nagy A, Semenkovich CF, Gordon JL. The gut microbiota as an environmental factor that regulates fat storage. *Proceedings of the National Academy of Sciences of the United States of America* 2004; 101(44): 15718-15723.
43. Brown R, Imran SA, Belsham DD, Ur E, Wilkinson M. Adipokine gene expression in a novel hypothalamic neuronal cell line: resistin-dependent regulation of fasting-induced adipose factor and SOCS-3. *Neuroendocrinology* 2007; 85(4): 232-241.
44. Imran SA, Brown RE, Wilkinson M. Tissue-specific effects of valsartan on rsn and fiaf gene expression in the ob/ob mouse. *Diabetes & vascular disease research* 2010; 7(3): 231-238.
45. Kim HK, Youn BS, Shin MS, Namkoong C, Park KH, Baik JH, Kim JB, Park JY, Lee KU, Kim YB, Kim MS. Hypothalamic Angptl4/Fiaf is a novel regulator of food intake and body weight. *Diabetes* 2010; 59(11): 2772-2780.
46. Kersten S. Regulation of lipid metabolism via angiopoietin-like proteins. *Biochemical Society transactions* 2005; 33(Pt 5): 1059-1062.
47. Wiesner G, Morash BA, Ur E, Wilkinson M. Food restriction regulates adipose-specific cytokines in pituitary gland but not in hypothalamus. *The Journal of endocrinology* 2004; 180(3): R1-6.
48. Yoon JC, Chickering TW, Rosen ED, Dussault B, Qin Y, Soukas A, Friedman JM, Holmes WE, Spiegelman BM. Peroxisome proliferator-activated receptor gamma target gene encoding a novel angiopoietin-related protein associated with adipose differentiation. *Molecular and cellular biology* 2000; 20(14): 5343-5349.
49. Stapleton CM, Joo JH, Kim YS, Liao G, Panettieri RA, Jr., Jetten AM. Induction of ANGPTL4 expression in human airway smooth muscle cells by PMA through activation of PKC and MAPK pathways. *Experimental cell research* 2010; 316(4): 507-516.
50. Lei X, Shi F, Basu D, Huq A, Routhier S, Day R, Jin W. Proteolytic processing of angiopoietin-like protein 4 by proprotein convertases modulates its inhibitory effects on lipoprotein lipase activity. *The Journal of biological chemistry* 2011; 286(18): 15747-15756.
51. Ge H, Yang G, Huang L, Motola DL, Pourbahrami T, Li C. Oligomerization and regulated proteolytic processing of angiopoietin-like protein 4. *The Journal of biological chemistry* 2004; 279(3): 2038-2045.
52. Yau MH, Wang Y, Lam KS, Zhang J, Wu D, Xu A. A highly conserved motif within the NH2-terminal coiled-coil domain of angiopoietin-like protein 4 confers its inhibitory effects on lipoprotein lipase by disrupting the enzyme dimerization. *The Journal of biological chemistry* 2009; 284(18): 11942-11952.
53. Yin W, Romeo S, Chang S, Grishin NV, Hobbs HH, Cohen JC. Genetic variation in ANGPTL4 provides insights into protein processing and function. *The Journal of biological chemistry* 2009; 284(19): 13213-13222.

54. Goh YY, Pal M, Chong HC, Zhu P, Tan MJ, Punugu L, Lam CR, Yau YH, Tan CK, Huang RL, Tan SM, Tang MB, Ding JL, Kersten S, Tan NS. Angiopoietin-like 4 interacts with integrins beta1 and beta5 to modulate keratinocyte migration. *The American journal of pathology* 2010; 177(6): 2791-2803.
55. Goh YY, Pal M, Chong HC, Zhu P, Tan MJ, Punugu L, Tan CK, Huang RL, Sze SK, Tang MB, Ding JL, Kersten S, Tan NS. Angiopoietin-like 4 interacts with matrix proteins to modulate wound healing. *The Journal of biological chemistry* 2010; 285(43): 32999-33009.
56. Mandard S, Zandbergen F, Tan NS, Escher P, Patsouris D, Koenig W, Kleemann R, Bakker A, Veenman F, Wahli W, Muller M, Kersten S. The direct peroxisome proliferator-activated receptor target fasting-induced adipose factor (FIAF/PGAR/ANGPTL4) is present in blood plasma as a truncated protein that is increased by fenofibrate treatment. *The Journal of biological chemistry* 2004; 279(33): 34411-34420.
57. Mandard S, Zandbergen F, van Straten E, Wahli W, Kuipers F, Muller M, Kersten S. The fasting-induced adipose factor/angiopoietin-like protein 4 is physically associated with lipoproteins and governs plasma lipid levels and adiposity. *The Journal of biological chemistry* 2006; 281(2): 934-944.
58. Sukonina V, Lookene A, Olivecrona T, Olivecrona G. Angiopoietin-like protein 4 converts lipoprotein lipase to inactive monomers and modulates lipase activity in adipose tissue. *Proceedings of the National Academy of Sciences of the United States of America* 2006; 103(46): 17450-17455.
59. Xu A, Lam MC, Chan KW, Wang Y, Zhang J, Hoo RL, Xu JY, Chen B, Chow WS, Tso AW, Lam KS. Angiopoietin-like protein 4 decreases blood glucose and improves glucose tolerance but induces hyperlipidemia and hepatic steatosis in mice. *Proceedings of the National Academy of Sciences of the United States of America* 2005; 102(17): 6086-6091.
60. Grootaert C, Van de Wiele T, Verstraete W, Bracke M, Vanhoecke B. Angiopoietin-like protein 4: health effects, modulating agents and structure-function relationships. *Expert review of proteomics* 2012; 9(2): 181-199.
61. Pal M, Tan MJ, Huang RL, Goh YY, Wang XL, Tang MB, Tan NS. Angiopoietin-like 4 regulates epidermal differentiation. *PloS one* 2011; 6(9): e25377.
62. Zhu P, Goh YY, Chin HF, Kersten S, Tan NS. Angiopoietin-like 4: a decade of research. *Bioscience reports* 2012; 32(3): 211-219.
63. Noh JM, Shen C, Kim SJ, Kim MR, Kim SH, Kim JH, Park BH, Park JH. Interleukin-1beta increases Angptl4 (FIAF) expression via the JNK signaling pathway in osteoblastic MC3T3-E1 cells. *Experimental and clinical endocrinology & diabetes : official journal, German Society of Endocrinology [and] German Diabetes Association* 2015; 123(8): 445-460.
64. Shaulian E, Karin M. AP-1 as a regulator of cell life and death. *Nature cell biology* 2002; 4(5): E131-136.